SCIENCE CHINA
Earth Sciences

SPECIAL TOPIC: Continental Subduction Zones
• REVIEW •

October 2015 Vol.58 No.10: 1679–1699
doi: 10.1007/s11430-015-5148-9

The Dabie-Sulu orogenic peridotites: Progress and key issues

CHEN Yi[1,2*], SU Bin[1] & GUO Shun[1,2]

[1] *State Key Laboratory of Lithospheric Evolution, Institute of Geology and Geophysics, Chinese Academy of Sciences, Beijing 100029, China;*
[2] *CAS Center for Excellence in Tibetan Plateau Earth Sciences, Beijing 100101, China*

Received December 7, 2014; accepted May 26, 2015; published online July 24, 2015

Orogenic peridotites in the Dabie-Sulu orogenic belt are commonly subdivided into 'crustal' type and 'mantle' type. They exhibit distinct mineral textures, metamorphic evolution, and whole-rock and mineral compositions. Most 'mantle' type peridotites originated from the subcontinental lithospheric mantle (SCLM) of the North China Craton and thus provide direct evidence of crust-mantle interactions in the continental subduction channel. In garnet peridotites, both garnet and Cr-spinel can be equilibrated at peak pressure conditions. Their stabilities are mainly controlled by the refertilized degree of whole-rock; therefore, spinel composition cannot be used to discriminate the partial melting degree of orogenic peridotites. Refractory mantle-derived dunites contain the textures of low Mg and high Ca olivine veins that crosscut orthopyroxene porphyroblasts, which is considered as evidence for silica-undersaturated melt-rock reactions. Such reactions occurring before subduction may potentially affect Re-Os isotopic compositions. Rutile, Ti-clinohumite and zircon in mantle-derived peridotites or pyroxenites provide direct mineralogical evidence for the transport of high field strength elements (HFSEs) from the subducted crust into the mantle wedge. Based on detailed *in situ* element and isotope analyses, we can constrain the source of metasomatic agents, the metasomatic time and the process of mass transfer. The mantle wedge above continental subduction zones has a wide range of oxygen fugacity values (FMQ=–5.50–1.75), showing a roughly negative correlation with the subducted depths. However, the calculated results of oxygen fugacity are significantly affected by mineral assemblages, *P-T* conditions and dehydrogenation-oxidation of nominally anhydrous mantle olivine during exhumation. Although significant progress has been made in the study of orogenic peridotites in the Dabie-Sulu orogenic belt, many critical questions remain. With new approaches and advanced technologic applications, additional knowledge of the phase relation in the peridotite-pyroxenite complex system, the mantle geodynamic process before continental subduction, the effects of crustal metasomatism on chemical composition, the oxygen fugacity, and the physical properties of the mantle wedge is anticipated.

garnet peridotite, subduction channel, subduction zone fluids/melts, crust-mantle interaction, oxygen fugacity

Citation: Chen Y, Su B, Guo S. 2015. The Dabie-Sulu orogenic peridotites: Progress and key issues. Science China: Earth Sciences, 58: 1679−1699, doi: 10.1007/s11430-015-5148-9

Garnet peridotites commonly occur as lenses, blocks or layers within high- to ultrahigh-pressure (HP-UHP) granitic/pelitic gneisses in continental subduction-collision zones. These peridotites are generally called 'alpine-type peridotites' or 'orogenic peridotites' (Menzies et al., 2001; Medaris et al., 2005). Compared to the country rocks, these orogenic peridotites not only preserve mineralogical evidence for subduction-related UHP metamorphism (>180–200 km) but also preserve plenary metamorphic evidence for mantle geodynamic processes prior to continental subduction (Zhang et al., 2000; Zheng et al., 2006b, 2014; Yang and Powell, 2008; Ye et al., 2009; Scambelluri et al., 2010). Therefore, although volumetrically minor, their geodynamic setting and UHP origin make orogenic mantle rocks an important window to the geodynamic processes of

*Corresponding author (email: chenyi@mail.iggcas.ac.cn)

continental subduction-exhumation, mantle evolution, and crust-mantle interaction in a regional scale with global geodynamic implications.

Several garnet peridotite and garnet-pyroxenite bodies occur as meter- to kilometer-sized blocks within the amphibolite-facies gneisses in the Dabie-Sulu UHP terrane (Figure 1). In the past twenty years, many petrological and geochemical investigations have been performed on these rocks, and significant progress has been made concerning their origins, metamorphic evolution and metasomatic processes (Zhang et al., 1995, 2000; Liou and Zhang, 1998; Yang and Jahn, 2000; Malaspina et al., 2006; Ye et al., 2009; Chen et al., 2013a, 2013b). Orogenic peridotites in the Dabie-Sulu collision zone were commonly classified into 'crustal' mafic-ultramafic cumulates and 'mantle' peridotites (Zhang et al., 2000; Zhang et al., 2009). The former was crystallized from mafic magmas that underwent magmatic differentiation in the lower continental crust prior to subduction, such as the Bixiling and the Maobei mafic-ultramafic complex (Zhang et al., 1995; Chavagnac and Jahn, 1996; Zhang R Y et al., 2006, 2010; Zhang Z M et al., 2006; Liu et al., 2008; Zheng et al., 2008). The latter originated from the mantle wedge above the slab and commonly records UHP metamorphism and metasomatism (Zhang R Y et al., 2004, 2009, 2011; Zheng et al., 2005b, 2006b, 2008; Yang et al., 2007; Zhao et al., 2007; Liu et al., 2012). These two types of orogenic peridotites exhibit significant difference in geochemical characteristics. Therefore, orogenic peridotites are usually classified into a Fe-Ti type and an Mg-Cr type based on their geochemical composition (Carswell et al., 1983). The Fe-Ti type corresponds to the 'crustal' peridotite, whereas the Mg- Cr type is consistent with the 'mantle' peridotite. Previous petrological and geochemical studies have indicated that most peridotites in the Dabie-Sulu orogenic belt belong to the 'mantle' type peridotite; they were scraped by the low- density continental crustal rocks along a subduction channel and exhumed back into the Earth's surface (Zheng, 2012).

The Dabie-Sulu orogenic peridotites experienced various degrees of metasomatism by fluids or melts derived from subducted continental crust and developed abundant metasomatic minerals. Therefore, orogenic peridotites and surrounding gneisses may represent a subducted slab-mantle interface (Zheng, 2012), making them the best samples in which to explore the physical chemistry effects of deep crust-mantle interaction in subduction zones (Chen et al., 2013d; Zheng and Hermann, 2014). In this paper, we briefly summarize mineralogical and petrological features, protolith affinity, geochemical characteristics, and crustal metasomatism of the Dabie-Sulu orogenic peridotites. We also suggest and discuss several key issues for the further study of orogenic peridotites.

1 Mineralogical and petrological characteristics of orogenic peridotites

Tens of localities of orogenic peridotites reported for the

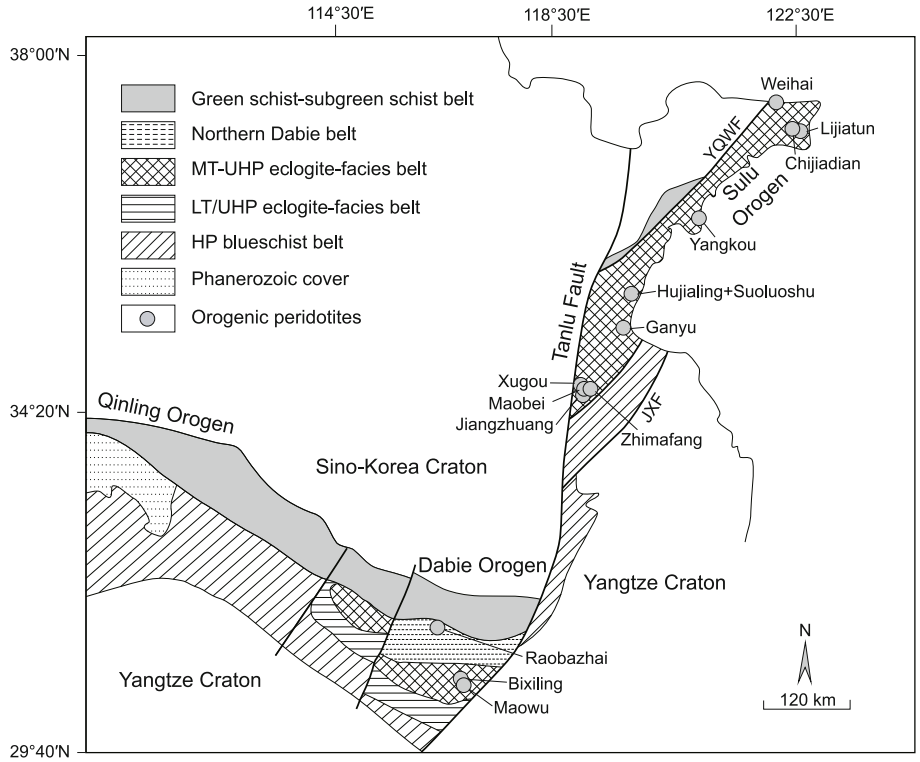

Figure 1 Sketched map showing the distribution of peridotites in the Dabie-Sulu orogen (modified after Zhang et al., 2009).

Dabie-Sulu UHP metamorphic belt (Figure 1). Most are exposed in the Sulu UHP metamorphic belt; only three peridotite bodies from Maowu, Bixiling, and Raobazhai are exposed in the Dabie UHP metamorphic belt. Except for the Maowu mafic-ultramafic complex, orogenic peridotites primarily consist of garnet lherzolite, with minor harzburgite, dunite and wehrlite, and are commonly associated with pyroxenite, eclogite, and amphibolite. They occur as meter- to kilometer-sized lenses or blocks in granitic/pelitic gneisses; a fault causes some of the peridotites to contact the surrounding gneisses (Xue et al., 1996; Zhang et al., 2009). Most of the basement gneisses are paragneisses (Zhang and Liou, 1998), which are usually enriched in biotite and epidote, and occasionally preserve garnet crystals. Apatite, rutile and zircon are common accessory minerals in the surrounding gneisses. Coesite inclusions were observed in the gneiss zircons, indicating that the basement gneisses also underwent UHP metamorphism (Ye et al., 2001). Several leucosomes were occasionally observed in the basement gneisses, reflecting partial melting processes (Zheng et al., 2011). Because of the extensive mylonitization and serpentinization at the boundary between peridotites and gneisses (Figure 2(a)), we hardly observe perfect modification textures of subducted crust-mantle interactions in this zone. Some phlogopite- and talc-rich layers occasionally occur at the contact boundary, most likely attributable to late-stage metasomatism by shallow crustal fluids. However, the inner part of the peridotite body is relatively fresh, and most garnet and olivine grains have survived here. Coarse-grained orthopyroxene porphyroblasts are very common in fresh orogenic peridotites. Furthermore, pyroxene-, phlogopite-, amphibole-, and Ti-clinohumite-rich, millimeter- to decimeter-thick veins occasionally crosscut the orogenic peridotites (Figure 2(b)–(d)). These veins provide direct samples in which to explore the crust-mantle interactions in continental subduction zones.

1.1 Petrological differences between continental and oceanic subduction zone peridotites

Orogenic peridotites occur both in continental and oceanic subduction zones, and all of them may contain evidence of crustal metasomatism. However, the systematic discrepancies of subducted material, fluid activities, and geothermal gradients between continental and oceanic subduction zones most likely cause significant petrological and geochemical differences in these subduction zone peridotites (Zheng et al., 2013). Thus, the crust-mantle interaction processes in continental and oceanic subduction zones may differ.

The most striking feature of oceanic subduction zone peridotites is their significant serpentinization. Most originated from the cold and hydrated mantle wedge just above

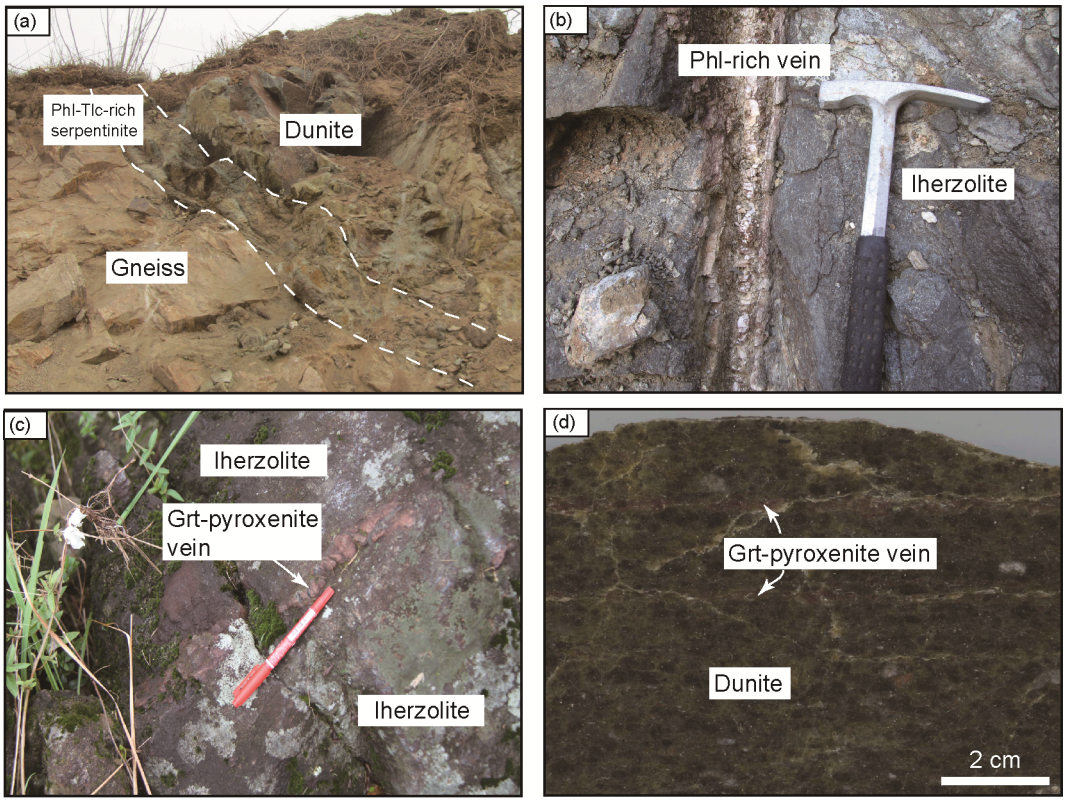

Figure 2 Photograph of the Dabie-Sulu orogenic peridotites in outcrop and hand specimen. (a) Phlogopite-talc-rich serpentine layer along the contact boundary between dunite and gneiss, Lijiatun. (b) Phlogopite-rich vein developed in the host lherzolite, Raobazhai. (c) Garnet pyroxenite vein occurring in garnet lherzolite, Bixiling. (d) Garnet pyroxenite vein cutting dunite, Maowu.

subducted slabs (Guillot et al., 2001, 2009; Savov et al., 2005, 2007), but a few may have originated from the cold and hydrated lithospheric mantle beneath the subducted oceanic crust (Chalot-Prat et al., 2003; Li et al., 2004). The serpentinized peridotites in oceanic subduction zones usually contain eclogite and blueschist blocks of various sizes and display an important role in the exhumation of oceanic mafic crust (Guillot et al., 2001; Agard et al., 2009; Chen and Ye, 2013). Serpentinized harzburgite is the dominant lithology, with minor clinopyroxene-poor lherzolite and dunite. Because they are moderately depleted in major element compositions and represent shallow parts (<80 km) of oceanic subduction zones, they are mostly spinel-facies peridotites. Garnet peridotites have been rarely reported in oceanic subduction complexes (Enami et al., 2004; Abbott et al., 2007; Hattori et al., 2010b). Therefore, oceanic subduction zone peridotites can only record the information of crust-mantle interactions at shallow depths. The metasomatic minerals in oceanic subduction zone peridotites are primarily low-temperature hydrous minerals such as serpentine, amphibole, chlorite, talc, and phlogopite. Several oceanic subduction zone peridotites occasionally preserve mineralogical evidence of serpentine dehydration and secondary olivine formation (Scambelluri et al., 2001, 2004; Nozaka, 2003; Padrón-Navarta et al., 2011; Spandler and Pirard, 2013). Such prograde metamorphic olivine is typically extremely Mg-rich, with Fo ranging from 94 to 99 (Li et al., 2004; Song et al., 2009; Arai et al., 2012). However, chlorite can be stable under peak metamorphic conditions, indicating that the metamorphic temperatures of the peridotites range from 650 to 800°C (Fumagalli and Poli, 2005; Padrón-Navarta et al., 2010). The fluids derived from serpentine dehydration are important carriers of Cl, Li, B, As, Sb, Sr, Pb, Cs, and U into subduction zones and are also important in the formation of forearc and arc magmatism (John et al., 2011; Kendrick et al., 2011; Kodolányi et al., 2012; Spandler and Pirard, 2013; Scambelluri et al., 2014). Ti-clinohumite-rich veins commonly occur in the peridotites with serpentine dehydration, implying that the fluids can partially transport HFSEs. The source of HFSEs may be derived from subducted oceanic crust or some Ti-rich phases (clinopyroxene and spinel) in oceanic subduction zone peridotites (Rebay et al., 2012; Arai et al., 2012).

Orogenic peridotites in continental subduction zones are entirely garnet peridotites. Most have lower loss-on-ignition (LOI: water dominated total volatiles; <5wt%) relative to oceanic subduction zone peridotites, reflecting weaker serpentinization. Although some continental subduction zone peridotites also show strong serpentinization (LOI>10wt%) (Xie et al., 2013), the serpentine currently circumfuses or crosscuts the matrix olivine and pyroxene and the symplectites after the peak garnet and Ti-clinohumite (Chen et al., 2013a). This feature indicates that the serpentinization of orogenic garnet peridotites is related to the fluid metasomatism at shallow crustal levels. Compared to oceanic subduction zone peridotites, those in continental subduction zones exhibit relatively fertile major element compositions; the peak mineral assemblage is mostly garnet+clinopyroxne+orthopyroxene+olivine+Cr-spinel±phlogopite±Ti-clinohumite (Zhang et al., 2000, 2009). Most orogenic garnet peridotites underwent UHP metamorphism (3.5–6.5 GPa), corresponding to a 100–200 km mantle depth. Exsolution lamellae are typical textures in orogenic garnet peridotites. For example, olivines from the Maowu and the Zhimafang garnet peridotites develop abundant exsolution lamellae of Fe-Ti oxides, most likely indicating that they were once subducted into very deep mantle (>300 km) (Dobrzhinetskaya et al., 1996). Traditional geothermobarometries and phase modeling yield the peak pressures of orogenic garnet peridotites that can be up to 6–7 GPa (Yang and Jahn, 2000; Ye et al., 2009; Chen et al., 2013a), also implying that they once reached a deep mantle of >200 km. Therefore, orogenic garnet peridotites in continental subduction zones are ideal for providing information on deep crust-mantle interactions. Except for the Raobazhai peridotite, almost all of the Dabie-Sulu orogenic peridotites preserve peak temperatures of <850°C. The Maowu, the Zhimafang, and the Xugou peridotites/pyroxenites record the peak *P-T* conditions corresponding to a very low subducted geothermal gradient (<5°C/km) (Yang and Jahn, 2000; Zhang et al., 2007; Ye et al., 2009; Spengler et al., 2012; Chen et al., 2013a), which is significantly lower than in oceanic subduction zones (Guillot et al., 2009; Chen et al., 2013c, 2013e).

Orogenic garnet peridotites and pyroxenites are commonly characterized by their complex metasomatic processes. They typically exhibit multistage and various metasomatic minerals, such as garnet, rutile, Ti-clinohumite, Ti-chondrodite, pyroxene, amphibole, phlogopite, epidote, sapphirine, magnesite, dolomite, apatite, monazite, celestite, karstenite, zircon and pyrite (Yang and Jahn, 2000; Zhang et al., 2000, 2007; Yang, 2003; Malaspina et al., 2006, 2009a; Ye et al., 2009; Chen et al., 2013a, 2013b). It is widely accepted that continental subduction usually follows oceanic subduction (Song et al., 2009). Therefore, the mantle wedge overlying the subducted continental slab most likely underwent multistage metasomatism from oceanic subduction to continental subduction processes. The metasomatic agents are expected to include melts from asthenospheric mantle, melts or fluids derived from subducted oceanic crust, and aqueous fluids or hydrous melts released from continental crust during subduction or exhumation (Zhang et al., 2005a, 2007; Zheng et al., 2006a, 2014; Ye et al., 2009; Chen et al., 2013a). Generally, two main types of metasomatism have been identified: modal (or patent) metasomatism and cryptic metasomatism (Malaspina et al., 2006; Scambelluri et al., 2006; Zhang et al., 2007; Vrijmoed et al., 2013). Modal metasomatism changes the modal compositions via the introduction of amphibole, chlorite, phlogopite, Ti-clinohumite, carbonate, ilmenite, rutile or zircon at the expense (or not) of the primary minerals

(olivine, pyroxene, spinel/garnet) in peridotites, whereas cryptic metasomatism only results in changes in the primitive mineral composition without the formation of new phases (Zhang et al., 2005a, 2007; Beyer et al., 2006; Malaspina et al., 2006; Zhao et al., 2007; Zhang Z M et al., 2011). Distinguishing these metasomatic processes requires detailed petrographic observations and *in situ* geochemical analyses.

1.2 Spinel-garnet transition (SGT) reaction

The Dabie-Sulu orogenic peridotites both in the 'crust' and the 'mantle' types are mostly garnet-facies peridotite. Only the Raobazhai ultramafic body is spinel-facies peridotite, representing a shallow origin (<80 km) that did not experience UHP metamorphism. Tsai et al. (2000) argued that the symplectite of spinel+clinopyroxene+orthopyroxene in the Raobazhai peridotite may have been formed by the decomposition of the primary garnet. However, the local bulk composition of the symplectite exhibits higher Cr_2O_3, CaO, and Na_2O and lower SiO_2 contents relative to the normal composition of garnet in peridotite. Notably, both garnet and spinel peridotites are currently associated with garnet pyroxenites. In garnet peridotites, Cr-spinel typically occurs as inclusions in the peak garnet and pyroxene or as matrix phases showing an equilibrium texture with other minerals (garnet, pyroxene, and olivine). This feature demonstrates that Cr-spinel (or chromite) can be stable under peak pressure conditions. A typical feature of the Cr-spinels in the Dabie-Sulu orogenic peridotites is their high $Cr^{\#}$ (=Cr/(Cr+Al)>0.60) (Zheng et al., 2005b, Chen et al., 2006a; Ye et al., 2009; Xie et al., 2013; Chen et al., 2013a). Generally, the stabilities of garnet and spinel, as well as their $Cr^{\#}$ values, are closely related to bulk-rock $Cr^{\#}$ and *P-T* conditions (Klemme et al., 2009; Ziberna et al., 2013). Cr is a compatible element and relatively immobile in mantle peridotite. Except for chromitite-bearing peridotites, the Cr contents of most mantle peridotites are not significantly different. However, Al is a relatively mobile element and is preferentially incorporated into a melt (Griffin et al., 2009). Therefore, mantle peridotites refertilized to different degrees show a significant discrepancy in Al_2O_3 content. In this regard, the stabilities and compositions of garnet and spinel would be directly controlled by the bulk Al_2O_3 content.

Both garnet and Cr-spinel are major Al-rich minerals in orogenic garnet peridotites. A peridotite with very low Al_2O_3 content (e.g., depleted dunite) cannot develop garnet even under UHP conditions; accordingly, the spinel in this rock is expected to have very high $Cr^{\#}$ values. However, a lherzolite with very high Al_2O_3 content, which is attributed to refertilization, would form garnet at relatively low pressures. The spinel in the lherzolite would have relatively low $Cr^{\#}$ values. For example, two types of peridotites have been identified in the Chinese Continental Scientific Drilling (CCSD) PP3 (Ganyu): one is fertile garnet peridotite with a high Al_2O_3 content; another is garnet-free peridotite that is depleted in Al_2O_3 (Yang et al., 2009). The Dabie-Sulu orogenic peridotites contain minor chromite-bearing dunites associated with garnet harzburgites or lherzolites. Their peak pressure conditions do not significantly differ. However, chromite in the depleted dunites has a $Cr^{\#}$ as high as 0.85–0.90, whereas Cr-spinel in the fertile garnet harzburgites/lherzolites has a relatively lower $Cr^{\#}$ of 0.60–0.85 (Zheng et al., 2005b, Chen et al., 2006a; Ye et al., 2009; Xie et al., 2013; Chen et al., 2013a).

Generally, increasing $Cr^{\#}$ in spinel is typically caused by (1) a high degree of partial melting; (2) silica-undersaturated melt-peridotite reaction; and (3) an SGT reaction. Al prefers to incorporate into melt, but Cr usually is retained in the residual peridotite, and a high-degree partial melting would consequently result in an increase of $Cr^{\#}$ in spinel. Thus, the spinel $Cr^{\#}$ is a good indicator of the depleted degree or formation temperature (Dick and Bullen, 1984; Kubo, 2002). Pyroxene usually has higher Cr contents than the equilibrated olivine. As a consequence of the silica-undersaturated melt-peridotite reaction in an open system in which the residual melt is lost from a peridotite, Cr is most likely shifted from the previous pyroxene into the secondary spinel because it is difficult for the newly formed olivine to store such high Cr contents (Morgan and Liang, 2005; Xu et al., 2008; Tursack and Liang, 2012). However, in a closed system in which the residual melt is retained in the peridotite, the $Cr^{\#}$ of the secondary spinel may decrease because melts always have a very low Cr content and $Cr^{\#}$. In the stability fields of garnet and spinel, their compositions are mainly controlled by the reactions as follows: $MgAl_2O_4$ (spinel)+$2Mg_2Si_2O_6$(orthopyroxene) = $Mg_3Al_2Si_3O_{12}$ (garnet) +Mg_2SiO_4 (olivine); (Fe, Mg)Cr_2O_4 (spinel)+2(Mg, Fe)$_2Si_2O_6$ (orthopyroxene) = (Mg, Fe)$_3Cr_2Si_3O_{12}$ (garnet)+(Mg, Fe)SiO_4 (olivine) (Brey et al., 1999, 2008; Girnis et al., 2003; Klemme, 2004). With a pressure increase, the spinel $Cr^{\#}$ will also increase (Figure 3) (Brey et al., 1999, 2008). However, in the stability field of garnet without spinel, the garnet $Cr^{\#}$ does not significantly change (Figure 3(c), (d)). Therefore, the spinel $Cr^{\#}$ in spinel peridotites is closely related to the formation temperature or the melt-rock reaction processes, whereas the spinel $Cr^{\#}$ in garnet peridotites is mainly controlled by pressure (Figure 3(a), (b)). Thus, some discrimination diagrams for spinel that are commonly used to show the degrees of partial melting cannot be applied in garnet peridotites.

Although many experimental studies have been focused on the SGT reaction, most of them were performed in simple CMAS and NCMAS systems (O'Neill, 1981; Gasparik and Newton, 1984; Klemme and O'Neill, 2000; Walter et al., 2002). The effect of bulk rock $Cr^{\#}$ on the SGT reaction has only been considered in a few studies (Klemme, 2004; Klemme et al., 2009). An increase in bulk rock Fe^{2+} content corresponding to an $Mg^{\#}$ decrease would decrease the

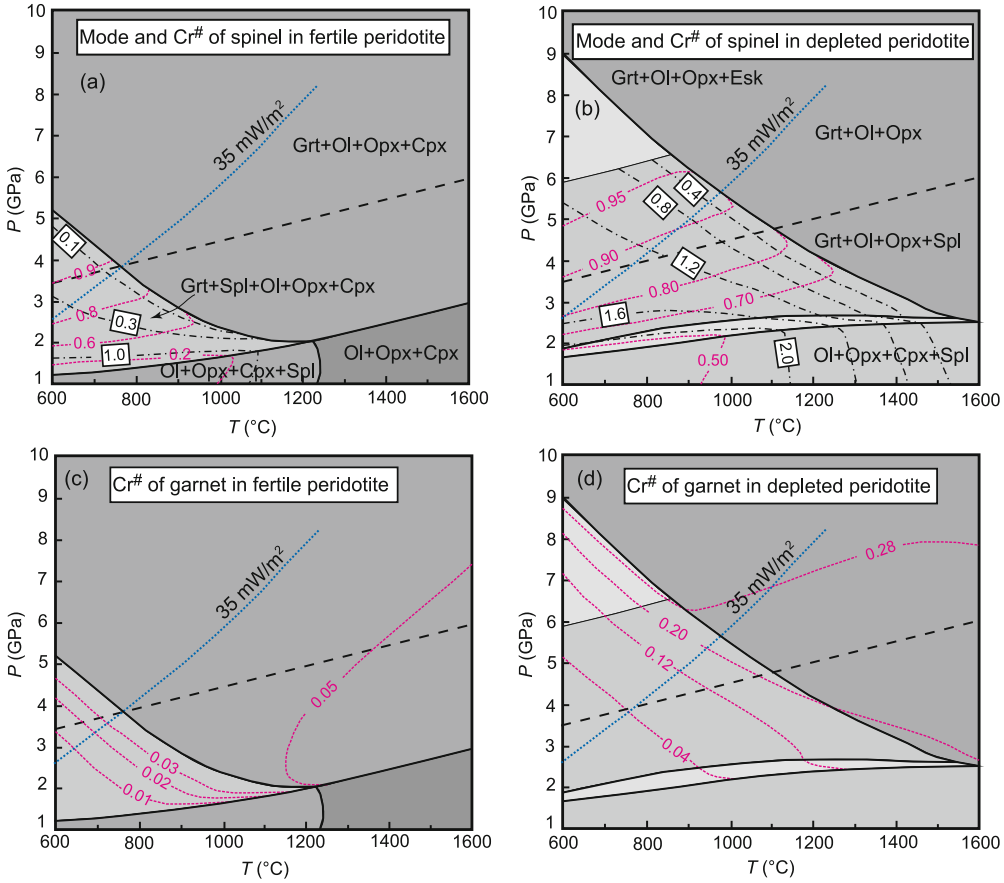

Figure 3 Phase equilibrium relations for fertile and depleted mantle peridotites in the system NCFMACrS (Na_2O-CaO-FeO-MgO-Al_2O_3-Cr_2O_3-SiO_2) (modified after Ziberna et al., 2013). (a) Spinel modal and $Cr^{\#}$ isopleths for fertile peridotite (Al_2O_3=4.85wt%, CaO=4.08wt%); (b) spinel modal and $Cr^{\#}$ isopleths for depleted peridotite (Al_2O_3=1.82wt%, CaO=0.29wt%); (c) $Cr^{\#}_{Grt}$ isopleths for fertile peridotite with the same composition as (a); (d) $Cr^{\#}_{Grt}$ isopleths for depleted peridotite with the same composition as (b). The dark dashed line represents the transition reaction between diamond and graphite. The whole-rock compositions of peridotites are collected from Ziberna et al. (2013). Grt, garnet; Opx, orthopyroxene; Cpx, clinopyroxene; Spl, spinel; Ol, olivine; Esk, eskolaite.

stability field of spinel and shift garnet-in into lower pressures (O'Neill, 1981). However, an increase of bulk rock Fe^{3+} and Cr contents would expand the stability fields of spinel and shift garnet-in into higher pressures (Figure 3) (O'Neill, 1981; Doroshev et al., 1997). Therefore, the SGT reaction is controlled by not only bulk $Cr^{\#}$ but also bulk $Mg^{\#}$ and $Fe^{3+}/\sum Fe$ (or oxygen fugacity). Because orogenic peridotites commonly underwent various degrees of crustal metasomatism, which is expected to modify bulk rock composition and oxygen fugacity, the composition of garnet and spinel in orogenic peridotites should be carefully considered based on the bulk rock composition and oxygen fugacity.

Petrological investigations on orogenic peridotites commonly show large errors in *P-T* estimation and significant discrepancies in *P-T* paths, even in a single peridotite body, such as the Zhimafang garnet peridotite (Yang and Jahn, 2000; Zhang R Y et al., 2008; Ye et al., 2009). Orogenic peridotites usually contain multistage garnet, orthopyroxene, and clinopyroxene, and it is difficult for these minerals to reach equilibrium, making their *P-T* estimation difficult. Until now, *P-T* conditions of orogenic peridotites were commonly calculated using garnet-clinopyroxene thermometers and garnet-orthopyroxene thermobarometers, which only consider the Fe-Mg-Al exchanges and neglect the Cr component. How to choose the garnet and pyroxene composition is a key issue in *P-T* estimation. Although several studies calculated the *P-T* conditions of orogenic peridotites based on the trace element partition between garnet and clinopyroxene (Zhang et al., 2010), they only yielded semi-quantitative results. However, the orthopyroxene-clinopyroxene REE thermometer can effectively overcome the limitations that the Fe-Mg-Al components in orogenic peridotites are easily modified or re-equilibrated during post-peak alterations or metasomatism (Liang et al., 2013; Sun and Liang，2014). Thermodynamic modeling research on ultramafic rocks is very rare, and only a few considered the effect of the Cr component on the phase equilibria. However, the stabilities of common metasomatic minerals such as amphibole, phlogopite, and Ti-clinohumite, as well as partial melting effects, are not well constrained in thermodynamic modeling (Figure 3). Precise constraint of *P-T* condi-

tions for orogenic peridotites should be based on careful understanding of phase equilibria in the complex Cr-bearing systems and composition evolution of garnet, spinel and pyroxene.

2 The protolith nature of orogenic peridotites

The two types of orogenic peridotites usually have different compositions and *P-T* evolution (Brueckner and Medaris, 2000; Reverdatto et al., 2008; Zhang C et al., 2011). The mantle type always indicates one-stage or multistage high-pressure metamorphism in the mantle interior (Brueckner et al., 2004; Spengler et al., 2006, 2012; Ye et al., 2009); it was scraped by the subducted or exhumed continental crusts into the subduction channel and underwent UHP metamorphism (Scambelluri et al., 2008; Zheng, 2012). Except for the exhumation process back to the crust, most processes in the mantle type orogenic peridotites were completed in the mantle. However, some studies suggest that part of the mantle type orogenic peridotites once intruded into the shallow crust levels and underwent significant serpentinization (Yang and Jahn, 2000; Yang et al., 2013). The crustal peridotites were crystallized from mantle magmas that intruded into the lower continental crust prior to continental subduction and usually belong to plagioclase- or spinel-facies peridotites. They were subducted with the continental crust to form garnet peridotites and then exhumed back to the Earth's surface (Krogh and Carswell, 1995; Zhang et al., 1995; Zhang C et al., 2011).

Previous studies indicated that crustal peridotites and pyroxenites typically exhibit complex compositional layers in the outcrop. However, many experimental and natural sample studies have demonstrated that the mantle peridotites metasomatized by the slab-derived fluids or melts also showed complex compositional layers with various lithologies (e.g. Iizuka and Nakamura, 1995; Vrijmoed et al., 2006, 2013). Therefore, it is difficult to identify these two types of orogenic peridotites in a field outcrop. Furthermore, the crustal cumulative peridotites typically have mineral textures that are different from the mantle-derived peridotites. The crustal cumulative peridotites mainly comprise euhedral olivine and pyroxene grains with a well-developed cumulate texture. Euhedral or subeuhedral Cr-spinel grains usually occur as inclusions in olivines. It is worth noting that typical triple junction texture cannot be used to indicate fractional crystallization process, because orthopyroxenes and olivines from several mantle-derived peridotites formed under high-temperature conditions also show such texture (Figure 4(a)) (Tsai et al., 2000; Wang et al., 2005). However, porphyroblastic orthopyroxenes are rarely preserved in cumulative dunites but are universal in mantle-derived peridotites (Figure 4(b)), such as the peridotites from Zhimafang, Ganyu, Lijiatun, Chijiadian, Yangkou and Raobazhai. Such orthopyroxene porphyroblasts usually record the earliest metamorphism and develop clinopyroxene and chromite (or Cr-spinel) exsolution lamellae (Figure 4(d)), most likely resulting from early high-degree partial melting under high-temperature conditions.

Reverdatto et al. (2008) described geochemical criteria to distinguish the two types of peridotites even after the complex history they have been subjected to after their original emplacement. Compared to the crustal cumulative peridotites/pyroxenites, the mantle-derived peridotites/pyroxenites typically have higher MgO, Cr and Ni contents, but lower FeO, TiO_2, Zr, Nb, and REE contents (Reverdatto et al., 2008). However, to distinguish these two types of orogenic peridotites based on geochemical criteria, we should carefully consider the effect of crustal metasomatism on the bulk rock composition, especially the incompatible elements. For example, the formation of metasomatic phlogopite and amphibole in peridotites would increase the bulk LILE, LREE and HFSE contents (Ionov and Hofmann, 1995; van Achterbergh et al., 2001; Coltorti et al., 2004; Powell et al., 2004; Scambelluri et al., 2006). The formation of metasomatic apatite, zircon and Ti-clinohumite will most likely increase the bulk REE and HFSE contents (Chazot et al., 1996; Zenetti et al., 1999; Zhang et al., 2007; Zhang Z M et al., 2011). The Ni content was most likely lost from the mantle peridotites due to S-bearing melt metasomatism (Fleet et al., 1996; Hattori et al., 2010a). Low-temperature alteration under high oxygen fugacity conditions may result in Cr that is lost from the mantle peridotites (Haggerty, 1995; Griecoa et al., 2004; Mellini et al., 2005). Vrijmoed et al. (2013) investigated the Svartberget garnet peridotite from the northernmost ultrahigh-pressure domain in the Western Gneiss Region (WGR) and showed that a sequence of metasomatic reaction zones developed between the mantle wedge peridotite and the country migmatitic gneiss. In the context of such strong metasomatism, the Svartberget garnet peridotites are likely to simultaneously possess the compositional characteristics of depleted mantle and subducted crust and are even akin to crust-derived peridotite (Vrijmoed et al., 2013). Garnet pyroxenites are the metasomatic products between mantle peridotites and felsic melts or are the metamorphic products of late-stage cumulate that was crystallized from mafic magmas. Refractory orogenic harzburgites or dunites consist primarily of olivine, with minor orthopyroxene and spinel/garnet, and were subjected to the weakest metasomatism by crust-derived agents among orogenic peridotites. The mineral compositions (e.g., olivine) of the orogenic harzburgites/dunites would not notably change during later metamorphism related to subduction and exhumation because little element exchange would occur between the abundant olivine and the few other minerals. Therefore, harzburgites/dunites are the best samples from which to trace the origins of orogenic peridotites. However, recovering their protolith nature also requires excluding the effect of cryptic metasomatism (Zheng, 2012).

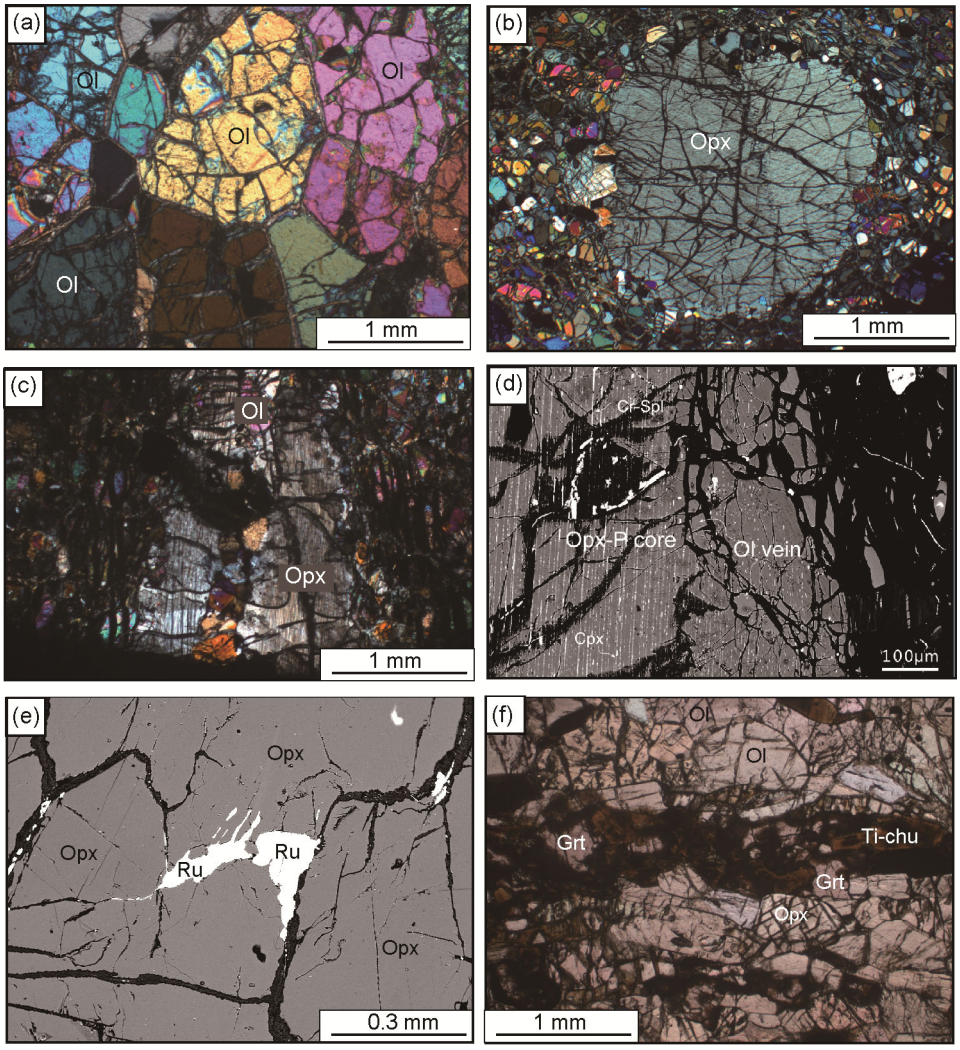

Figure 4 Microphotographs and Back-scattered electron images (BSE) showing mineral textures in the Dabie-Sulu orogenic peridotites. (a) 'Triple junction' texture in mantle-derived peridotite, Lijiatun; (b) coarse-grained orthopyroxene porphyroblast in mantle-derived peridotite, Lijiatun; (c) fine-grained olivine vein cutting orthopyroxene porphyroblast, Lijiatun; (d) chromite and clinopyroxene lamellae in the core of orthopyroxene porphyroblast that is cut by fine-grained olivine vein, Lijiatun; (e) rutile veins along the orthopyroxene boundaries, Maowu; (f) Ti-clinohumite-rich vein in harzburgite, Maowu.

The Dabie-Sulu orogenic peridotites, which were generated by different formation processes, are expected to have a wide compositional range. The mantle-derived peridotites commonly have higher $Mg^{\#}$ values (85.9–93.8), Ni contents (1441–2926 ppm), and Mg/Si ratios (1.04–1.83), whereas the crustal peridotites (such as the Maobei and the Bixiling peridotites) show relatively lower $Mg^{\#}$ values (<85), Ni contents (760–1440 ppm), and Mg/Si ratios (0.85–1.51) (Figure 5). In the garnet-facies peridotites, the Mg/Si ratio reflects the proportion of olivine/(pyroxene+garnet) because the Mg/Si ratio is 2 for olivine (Fo), 1 for orthopyroxene and garnet (Pyr), and 0.5 for clinopyroxene (Di). Thus, the Mg/Si ratio in orogenic peridotites can denote the degrees of refertilization. Figure 5 shows that the mantle-derived peridotites in the Dabie-Sulu orogen mostly have compositions similar to the Proterozoic subcontinental lithospheric mantle (SCLM). However, some orogenic mantle peridotites have compositions overlapping the Archean SCLM (Figure 5). Note that Si-rich melt metasomatism is expected to only generate orthopyroxene and would decrease the bulk rock Mg/Si ratios, but the bulk rock $Mg^{\#}$ values would not significantly change. However, the subducted crusts currently released Si-Al-rich and low Mg granitic melts during the early stage of exhumation. The mantle peridotites metasomatized by such melts are expected to develop metasomatic pyroxene and garnet (Malaspina et al., 2006, 2009a; Chen et al., 2013a), resulting in the decrease of both bulk rock Mg/Si and $Mg^{\#}$. Therefore, some Archean SCLM peridotites, which suffered extensional crustal metasomatism with granitic melts, most likely show the chemical characteristics of the Proterozoic SCLM. Notably, the bulk $Mg^{\#}$ cannot be the only criterion to distinguish the two types of orogenic peridotites. Some cumulative peridotites that were crystallized in the sub-arc mantle also have an $Mg^{\#}$ higher

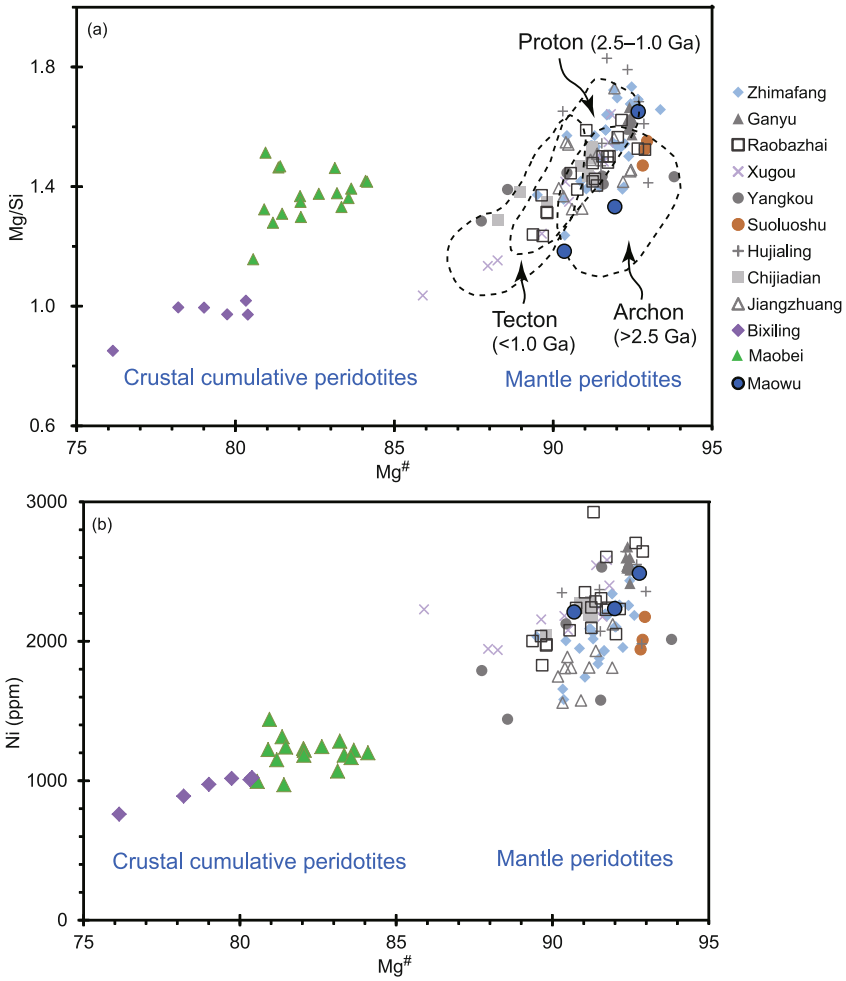

Figure 5 Diagrams of $Mg^{\#}$ vs. Mg/Si (a) and $Mg^{\#}$ vs. Ni (b) for the Dabie-Sulu orogenic peridotites. Zhimafang (CCSD-PP1) (Zhang et al., 2000, 2007; Yang, 2003; Yang et al., 2007, 2009); Maobei (CCSD-MH) (Liu et al., 2008; Yang et al., 2009; Zhang et al., 2010; Li et al., 2011); Ganyu (CCSD-PP3) (Yang et al., 2009; Raobazhai: Zhi et al., 2004; Zheng et al., 2008; Xugou: Yuan et al., 2007); Yangkou (Chen et al., 2002; Zhang et al., 2005b; Xie et al., 2013); Suoluoshu (Xie et al., 2013); Hujialing (Yang, 2006; Zhang R Y et al., 2011; Xie et al., 2013); Chijiadian (Zhang et al., 2000; Zhao et al., 2007); Jiangzhuang (Zhang et al., 2000; Zhang Z M et al., 2011); Bixiling (Chavagnac and Jahn, 1996; Zheng et al., 2008); Maowu (Jahn et al., 2003; Malaspina et al., 2006; Chen et al., 2013b). Arcton, Proton and Tecton fields are from Griffin et al. (1999).

than 90; however, these peridotites usually contain significantly lower Ni (<1000 ppm) relative to the normal mantle peridotites (Rajesh et al., 2013).

The platinum group element (PGE) is an effective approach to distinguish mantle and crustal orogenic peridotites. PGEs are generally subdivided into two groups: compatible IPGEs (Iridium-group PGE; Os, Ir, Ru) and incompatible PPGEs (Palladium-group PGE; Pd, Pt). IPGEs have been suggested as refractory and to preferentially enter residue during partial melting, whereas PPGEs are mainly concentrated in metal sulfides (e.g., pentlandite and chalcopyrite), which are released into the melt as soon as the sulfides begin to melt (Barnes et al., 1985; Lorand et al., 2013). If peridotites are subjected to metasomatism, the PPGE abundances will increase as PPGE-rich sulfides precipitate from the melts (Ackerman et al., 2013; Wang Z C et al., 2013). Until now, the PGE abundances were only reported in the peridotites from Raobazhai, Bixiling, Ganyu, Hujialing, Suoluoshu, and Yangkou (Chen et al., 2006b; Zheng et al., 2008; Liu et al., 2012; Xie et al., 2013). The mantle orogenic peridotites from Ganyu, Hujialing, Suoluoshu, and Yangkou have IPGE abundances similar to the primitive upper mantle (PUM; Becker et al., 2006). They also have high IPGE/PPGE and Ir/(Pt+Pd) ratios, consistent with the SCLM xenoliths in the North China Craton (Figure 6). However, because of partial melting, the PPGE contents show various degrees of depletion (Righter et al., 2004; Brenan et al., 2005; Chen et al., 2006b; Zheng et al., 2008; Xie et al., 2013). On the other hand, the Bixiling cumulative peridotite has relatively lower IPGE contents, with low IPGE/PPGE and Ir/(Pt+Pd) ratios, similar to other cumulative peridotites in different geological settings (Figure 6).

The two types of orogenic peridotites can also be distinguished based on the compositions of olivine and spinel. The olivines in the mantle-derived peridotites from the Dabie-Sulu orogen have high Fo values (generally >91) and

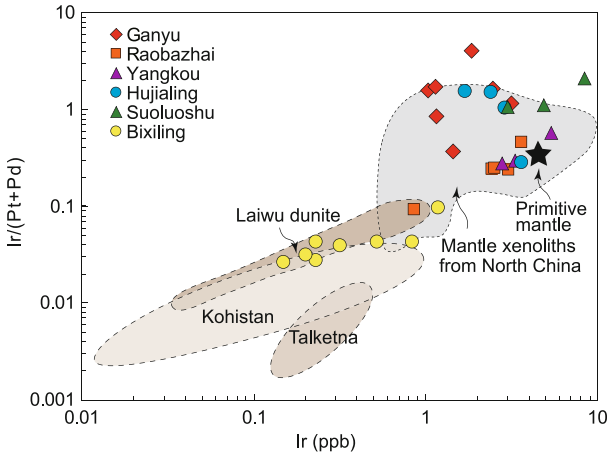

Figure 6 Diagram of Ir vs. Ir/(Pt+Pd) for the Dabie-Sulu orogenic peridotites. The whole-rock PGE data for the peridotites are from Ganyu (Chen et al., 2006b); Raobazhai (Zheng et al., 2008); Yangkou, Suoluoshu and Hujialing (Xie et al., 2013); Bixiling (Zheng et al., 2008; Liu et al., 2012). The whole-rock PGE data for the ancient mantle xenoliths from the North China Craton are from Gao et al. (2002), Zheng et al. (2005a), Becker et al. (2006), Zhang H F et al. (2008), Liu et al. (2010, 2011, 2014). The field for the Laiwu cumulative dunite is after Wang et al. (2012). The field of PGE data from the cumulative peridotites in the Kohistan and Talketna arc are after Hattori and Guillot (2007). Primitive mantle value is also shown with dark star (McDonough and Sun, 1995).

NiO contents (0.31wt%–0.45wt%), similar to those in refractory mantle peridotites (Tatsumi, 1986) and in the mantle peridotite xenoliths from the North China Craton (Zheng et al., 2006b, 2008, 2014; Xu et al., 2008). However, the olivines from the crustal type orogenic peridotites have relatively low Fo (<85) (Zheng et al., 2008), with typically lower Ni content and higher Ca, Ti, and Cr contents than the normal mantle olivines (Foley et al., 2013). Note that some olivines in the cumulative peridotites from the sub-arc mantle also have high Fo values (>90) and exhibit a rapid decrease in NiO contents from >0.5wt% to <0.1wt% without a significant change in Fo (Santos et al., 2002; Hattori et al., 2010b; Arai et al., 2012; Rajesh et al., 2013). Furthermore, the spinels from the cumulative peridotites feature a wide range of $Cr^{\#}$ and $Mg^{\#}$ values, but their $Mg^{\#}$ values are commonly lower than those from the mantle-derived peridotites (Arai et al., 2003; Bryant et al., 2007). Because both Cr and Ni are compatible elements, they are expected to be quickly removed from a melt into olivine and spinel during their solidification, resulting in a rapid decrease of these components in the residual melt (Melcher et al., 1997). Moreover, the spinel TiO_2 contents in the cumulative peridotites are typically higher (up to 0.8wt%) than those from the mantle-derived peridotites (Hattori et al., 2010b; Arai et al., 2012; Rajesh et al., 2013). Although the reactions between peridotite and silica-undersaturated basaltic melt can also increase the TiO_2 content in spinel from the mantle-derived peridotites (Pearce et al., 2000; Morgan and Liang, 2005), such spinel usually has a higher $Mg^{\#}$ than the cumulative spinel.

3 Silica-undersaturated melt-rock reactions

Melt-peridotite reactions are widespread in the upper mantle and are considered to be a key mechanism responsible for the chemical changes and physical property transformations of the ancient SCLM (Gao et al., 2002; Zhang et al., 2003; Shaw et al., 2006; Zheng, 2012; Tang et al., 2013). Based on the melt composition, the melt-peridotite reactions have been classified into two groups: (1) the reaction between the silica-rich melt and the refractory peridotite that is characterized by the partial replacement of olivine by pyroxene and consequently results in the transformation of refractory harzburgite or dunite to relatively fertile lherzolite or pyroxenite (McPherson et al., 1996; Rapp et al., 1999; Le Roux et al., 2007; Uysal et al., 2015); (2) the reaction between the silica-undersaturated melt and the pyroxene-rich (fertile) peridotite that preferentially converts pyroxene to olivine and leads to a modal shift towards dunite (Kelemen, 1990; Kelemen and Dick, 1995; Braun and Kelemen, 2002; Suhr et al., 2003). The silica-undersaturated melt (carbonitic melt or basaltic melt) is commonly considered to be derived from the asthenosphere (Piccardo and Vissers, 2007; Zheng, 2012) or from the lower part of lithospheric mantle (Ackerman et al., 2009). Such silica-undersaturated melt-peridotite reactions have been widely investigated in ophiolitic peridotites and peridotite xenoliths from the SCLM, but rarely reported in orogenic peridotites. Relative to peridotite xenoliths from the SCLM, orogenic peridotites appear to possess more information on the group (1) reaction because silica-rich melts are widespread in both oceanic and continental subduction zones.

The Dabie-Sulu orogenic peridotites commonly suffered multistage metasomatism by silica-rich fluids or hydrous melts derived from subducted continental crust (Zhang et al., 2007; Ye et al., 2009; Chen et al., 2013b), which makes distinguishing the silica-undersaturated melt-peridotite reactions difficult. However, parts of the Dabie-Sulu orogenic peridotites were most likely involved in the silica-undersaturated melt-peridotite reactions. For example, several orthopyroxene porphyroblasts in the garnet peridotites from the CCSD main hole were cut by fine-grained olivine veins (Li et al., 2011; Figure 3(d)), suggesting the formation of secondary olivine caused by the reaction between silica-undersaturated melt and orthopyroxene. We have observed a similar texture in several peridotites from the Dabie-Sulu orogen. The Lijiatun dunite also develops secondary olivine veins after orthopyroxene porphyroblasts (Figure 4(c), (d)). Relative to the matrix olivine, the secondary olivine grains have lower $Mg^{\#}$ values and higher CaO and TiO_2 contents (unpublished data), different from those in the residual peridotites that were generated by a partial melting process. During the reaction between silica-undersaturated melt and orthopyroxene, Ca and Ti are preferentially incorporated into secondary olivine (Thompson and Gibson, 2000), whereas Si is incorporated into the residual melt. Addition-

ally, Cr is a compatible element and would be retained in the olivine veins to form secondary Cr-spinel. Therefore, the secondary olivine formed by the melt-peridotite reaction has a lower $Mg^{\#}$ (controlled by the melt/rock ratio and the melt $Mg^{\#}$) and higher CaO and TiO_2 contents relative to the normal mantle olivine (Xu et al., 2008, 2010; Ackerman et al., 2013; Wang Z C et al., 2013; Yu et al., 2014). Note that the orthopyroxene porphyroblasts developing the secondary olivine veins are always surrounded by LREE- and LILE-enriched and HFSE-depleted clinopyroxene and pargasitic amphibole, which are considered to be the metasomatic products between orthopyroxene and slab-derived fluid or melt. This mineral texture indicates that the silica-undersaturated melt-peridotite reaction most likely took place prior to continental subduction/exhumation. Therefore, orogenic dunites cannot be simply considered as the residue after a high degree of partial melting of the lithospheric mantle. Orogenic lherzolites and pyroxenites, which have been subjected to intensive metasomatism by silica-rich melt/fluid during slab subduction/exhumation, are the most widely distributed lithologies and have received the most attention (Liou et al., 2004; Zhang et al., 2005a; Le Roux et al., 2007; Lorand et al., 2008; Ye et al., 2009). However, we should also attach greater importance to orogenic dunites or harzburgites that most likely record the silica-undersaturated melt-peridotite reactions in the SCLM.

The mantle-derived peridotites in the Dabie-Sulu orogen have similar mineral and whole-rock compositions to the Archean SCLM of the North China Craton. Yuan et al. (2007) suggested that the Xugou peridotite originated from the SCLM of the Yangtz Craton based on contrasting younger Paleoproterozoic Re-depletion ages (T_{DR}, 1.8–2.0 Ga) and Re-Os model ages (T_{MA}, 1.9–2.2 Ga). However, the $^{187}Os/^{188}Os$ data of the Raobazhai (Dabie) (Zheng et al., 2009) and the Xugou (Sulu) peridotites (Yuan et al., 2007) overlap the Os isotopic compositions of both the SCLMs of the Yangtz and the North China Craton. Three direct arguments favor the Dabie-Sulu mantle-derived peridotites derivation from the SCLM hanging wall of the North China Craton during the prograde evolution of a continental subduction zone. (1) The refractory peridotite chemistry with olivine $Fo_{91–93}$ is similar to that of the refractory mantle xenoliths inferred to be of Archean age in the North China Craton (Zheng et al., 2014). By contrast, the northern margin of the Yangtz Craton, which formed the footwall during the continent-continent collision, has a lower olivine $Fo_{88–91}$ (Zhang et al., 2001). (2) The mantle-derived orogenic peridotites are currently surrounded by continental supracrustal rocks but are not associated with continental lower crustal rocks. Thus, it is very difficult to use the SCLM of the Yangtz Craton to interpret the mantle source of orogenic peridotites. (3) The peak *P-T* conditions of the mantle-derived orogenic peridotites were constrained at 3.5–6.5 GPa and ~800°C (Yang and Jahn, 2000; Zhang R Y et al., 2005b, 2011; Spengler et al., 2012; Chen et al., 2013a), corresponding to the mantle wedge environment just above the subducted slab. However, the temperature is significantly lower than that of the Yangtz SCLM (Zhang et al., 2001). Notably, the Dabie-Sulu mantle-derived orogenic peridotites mostly show Paleoproterozoic T_{DR} and T_{MA} (Chen et al., 2006b; Yuan et al., 2007; Zheng et al., 2009). Re is a moderately incompatible element and is preferentially incorporated into melt, whereas Os is highly compatible with mantle residue. Numerous studies have shown that the Re-Os isotopic system is easily modified during the melt-peridotite reaction due to the breakdown of primary sulfides and reprecipitation from the reactive melt (Becker et al., 2001; Büchl et al., 2002; Ackerman et al., 2013; Wang Z C et al., 2013). The melt-peridotite reaction would increase Re abundance rapidly, which probably induced various increases of $^{187}Re/^{188}Os$ and $^{187}Os/^{188}Os$ (depending on the reaction age), thereby producing a much younger T_{RD} age than the actual melting age of the mantle peridotite. The available Re-Os isotopic data consistently yield Paleoproterozoic melting ages for the Dabie-Sulu mantle-derived orogenic peridotites (Chen et al., 2006b; Yuan et al., 2007; Zheng et al., 2009), which are slightly younger than the primary source of Archean SCLM in North China (Gao et al., 2002; Wu et al., 2006) and were previously attributed to the Triassic metasomatism caused by fluids or felsic melts from the subducting continental crust (Zheng et al., 2009; Zheng, 2012). Nevertheless, the refractory dunites that experienced weak metasomatism yield similar T_{RD} ages as those of the lherzolites/harzburgites (Chen et al., 2006b; Zheng et al., 2009), indicating that, except for the Triassic metasomatism, the silica-undersaturated melt-rock reactions prior to subduction may potentially affect the Re-Os isotopic compositions.

4 HFSE mobilization during crust-mantle interactions

Element exchange during crust-mantle interactions in the subduction factory is a key geochemical dynamic mechanism for mantle heterogeneity (Zheng, 2012). Most previous studies focused on the effect of crustal metasomatism on LREE and LILE modification in the mantle wedge rocks (e.g., Scambelluri et al., 2004, 2010; Malaspina et al., 2006, 2009a; Zhang et al., 2007; Miller et al., 2009; Spandler and Pirard, 2013). Only a few studies examined HFSE mobilization (Kalfoun et al., 2002; Garrido et al., 2005). Thus, the behavior of HFSEs during crust-mantle interactions in subduction zones is not well constrained. Some metasomatic minerals in the Dabie-Sulu orogenic peridotites, such as rutile, zircon, Ti-clinohumite, and Ti-chondrodite, are important HFSE carriers. These minerals directly provide mineral evidence for the HFSE mobilization from the subducted continental crust into the mantle wedge.

Rutile, Ti-clinohumite, and Ti-chondrodite are Ti-rich phases and commonly occur in garnet peridotites and pyroxenites (Kalfoun et al., 2002; Yang, 2003; Zhang et al., 2007; Rebay et al., 2012; Chen et al., 2013a). Petrological observations indicate that rutile and Ti-clinohumite always occur as fine-grained veins or layers (Figure 4(e), (f)), implying that their formation may be related to fluid/melt metasomatism. The rutile veins were interpreted as direct precipitation from a Ti-bearing fluid/melt (Kalfoun et al., 2002). However, Ti-clinohumite and Ti-chondrodite have similar Mg/Si ratios to olivine; thereby, they are produced by the reactions between the Ti-bearing agent and the olivine (Zhang et al., 2007). Until now, the phase relations among rutile, Ti-clinohumite and Ti-chondrodite in the ultramafic system are not well constrained because of the lack of suitable activity-composition models and thermodynamic data for Ti-clinohumite and Ti-chondrodite. In the Dabie-Sulu orogenic peridotites, Ti-clinohumite is the most common Ti-rich phase that is typically equilibrated with phlogopite, orthopyroxene, magnesite and garnet. This feature indicates that the metasomatic agent is not only enriched in Ti but also enriched in Si, Al, K, and CO_2 (Zhang et al., 2007, 2009, 2010). The garnet and orthopyroxene equilibrated with Ti-clinohumite mostly provide evidence of metamorphic pressures higher than 4.5 GPa, implying that the metasomatic process occurred under UHP conditions.

An HP-HT experimental study (Iizuka and Nakamura, 1995) that was conducted at 8 GPa and 800°C, showed that Ti-clinohumite- and orthopyroxene-rich layers were observed at the contact boundary between eclogite and dunite. This experimental result indicates that: (1) the Ti-clinohumite layer was produced by the metasomatic reaction between peridotite and a Ti-bearing fluid released from eclogite, and (2) Si and Ti show significant fractionation during the metasomatic process. Ti-clinohumite in the Dabie-Sulu orogenic peridotites currently contain various F, which shifts its stability field to higher temperature conditions (Trommsdorff et al., 2001). The F-bearing Ti-clinohumite indicates that the metasomatic agent is also an F-bearing fluid/melt that has a strong ability to mobilize HFSEs (Keppler, 1993; Rapp et al., 2010). Note that the Ti-clinohumites found in continental subduction zone peridotites may have different origins from those in oceanic subduction zone peridotites. In oceanic subduction zone peridotites, Ti-clinohumites commonly occur as lamellae in olivine and are interpreted to be Ti-clinohumite defects in OH- and Ti-bearing olivine (Shen et al., 2014). Several Ti-clinohumite veins also occur in oceanic serpentinized peridotites and are considered as metasomatic products formed by interactions between the pre-existing olivine and the Ti-bearing fluid (Arai et al., 2012; Rebay et al., 2012; De Hoog et al., 2014). However, the source of Ti in fluid is attributed to the Ti-bearing spinel and clinopyroxene in the peridotite interior (Arai et al., 2012; Rebay et al., 2012). The spinel and pyroxene in the continental subduction zone peridotites currently have very low Ti abundance, strongly suggesting that the Ti component in the metasomatic fluid/melt was sourced from other rocks. According to the metasomatic minerals, such as orthopyroxene, phlogopite and magnesite that are equilibrated with Ti-clinohumite, the metasomatic fluid/melt rich in Ti, Si, Al, K, F and CO_2 was most likely derived from the subducted continental crust (Zhang et al., 2009; Malaspina et al., 2006, 2009a) or an enriched mantle (Zhang et al., 2007).

Zircon in orogenic peridotites is also another important mineral that provides evidence for HFSE mobilization during crust-mantle interactions (Zheng, 2012). It enables us to constrain not only the source of the metasomatic agent but also the metasomatic age (Katayama et al., 2003; Zheng et al., 2003; Zhang et al., 2005a; Hermann et al., 2006; Zhang Z M et al., 2011; Zheng et al., 2014). Zircon grains have been separated from the peridotites from Zhimafang, Jiangzhuang, Chijiadian, Ganyu, Xugou, Raobazhai, Yangkou and Hujialing; some zircon grains can be observed in thin-section. Most zircon-bearing orogenic peridotites also contain abundant metasomatic minerals, such as phlogopite and Ti-clinohumite (Zhang Z M et al., 2011). The mineral inclusions in zircon mainly comprise apatite, with minor garnet, olivine, orthopyroxene, phlogopite, Ti-clinohumite and magnesite, indicating that the metasomatic fluid/melt contains P, Ti, LILEs, LREEs, and Zr. Most zircon grains are rounded and show no internal structure in BSE/CL images, but oscillatory zoning or anhedral relict cores remain in a few (Zheng et al., 2014). Metamorphic zircons record ages mostly in the range of 212–227 Ma (Zhang et al., 2005a; Zheng et al., 2006a, 2008; Yang et al., 2009; Zhang Z M et al., 2011), slightly younger than the UHP metamorphic age of 225–240 Ma (Zheng, 2012). Their Th/U ratios are 0.1–1.17 (Zhang et al., 2005a; Zhang Z M et al., 2011; Zheng et al., 2006a, 2008, 2014), demonstrating that the zircon grains in orogenic peridotites may be crystallized from hydrous melts released by the subducted continental crust during the early stages of exhumation (Zheng, 2012). Few zircon grains indicate old ages from the Proterozoic to the Archean (Yang et al., 2005, 2009; Liu F L et al., 2011; Zheng et al., 2014).

As we know, the primitive mantle is depleted in Zr and zircon cannot be directly crystallized from the depleted mantle. Zircon occurring in mantle peridotite commonly reflects metasomatism. The relict detrital zircon cores were physically extracted by the metasomatic agent from host UHP rocks during the slab-mantle interactions, with their origin from the subducting continental crust (Zheng, 2012). The occurrence of a coesite inclusion in the zircon from the Sulu garnet peridotite (Yang et al., 2003), as well as feldspar, quartz and felsic melt inclusions in the zircon from the Bohemian garnet peridotite (Liati and Gebauer, 2009), indicates that some crustal minerals were physically transported by the crust-derived melt into the mantle wedge peridotites and showed disequilibrium with the mantle minerals.

Hydrous melt commonly has higher viscosity than aqueous fluid and more likely transports the crustal material into the mantle wedge. During the slab-mantle interactions in the continental subduction channel, Si-Al-Na components would rapidly precipitate into the mantle wedge peridotites, resulting in a decrease of the Zr solubility of the metasomatic agent (Zotov and Keppler, 2000; Wilke et al., 2012; Louvel et al., 2013). The metamorphic growth of zircon occurred in the metasomatized peridotites when Zr became oversaturated in the crustal-derived melt. In the Dabie-Sulu orogenic peridotites, the zircons with U-Pb ages older than the Triassic most likely represent the following: (1) relict detrital zircons to be metamorphically recrystallized in the crustal-derived agent (Zheng, 2012; Zheng and Hermann, 2014); (2) newly formed zircons crystallized from the metasomatic melt derived from the asthenospheric mantle (Zheng et al., 2006a, 2014); or (3) early metamorphic zircons formed during the ancient oceanic slab-mantle interactions. Tracing the possible origins of these three types of zircon requires us to carefully distinguish. Therefore, to understand the zircon ages and sources as well as the mechanism of HFSE mobilization, we should investigate the textures of zircon and inclusions involved, zircon trace element and isotopic composition in detail.

5 Oxygen fugacity of the mantle wedge in continental subduction zones

The oxidation state of the Earth's mantle is reflected by its prevailing oxygen fugacity (fO_2). Some transitional metals (e.g., Fe^{2+} and Fe^{3+}) are very sensitive to oxygen fugacity. Thus, the $Fe^{3+}/\sum Fe$ ratio is an index parameter to reflect the oxygen fugacity of a rock (Christie et al., 1986; Kress and Carmichael, 1991). Metamorphic phase relations are affected by the bulk rock $Fe^{3+}/\sum Fe$ (or fO_2) (Rebay et al., 2010; Chen et al., 2013c). Accordingly, mineral assemblages and compositions can also reflect oxygen fugacity. fO_2 is commonly recorded by the Fe^{3+} contents of mafic minerals or V/Sc and Zn/Fe ratios of the whole-rock (Mattioli and Wood, 1986; Wood and Virgo, 1989; Ballhaus et al., 1991; Lee et al., 2005, 2010). The oxygen fugacity of subduction zone fluid or melt, an important issue in the study of the subduction factory, is closely related to subduction zone magmatism and mineralization (Sun et al., 2004; Lee et al., 2010). The crustal-derived C-O-H fluid or melt in subduction zones generally has variable fO_2, as shown by the occurrence of diamond, moissanite, CO_2 and CH_4 fluid inclusions in HP-UHP metamorphic rocks (Xu et al., 1992, 2003, 2005; Fu et al., 2003; Pan et al., 2003; Wang et al., 2007; Song et al., 2009). The variable fO_2 in crustal-derived fluid or melt is expected to be directly recorded by the metasomatic mantle minerals during the slab-mantle interactions and then pass the signature to the mafic magmas formed by partial melting of the metasomatized mantle wedge (McCammon et al., 2004). Therefore, study of mantle wedge fO_2 requires carefully considering the mixing effect of crustal metasomatism and following partial melting process.

The fO_2s of mid-ocean ridge basalts (MORB) and arc lavas have now been widely investigated. Relative to the fayalite-magnetite-quartz (FMQ) buffer, MORBs have $\triangle\log fO_2$ ($=\triangle FMQ=\log fO_2^{sample}-\log fO_2^{FMQ}$) values between −2 and 0 log units from the FMQ buffer (hereafter referred to as FMQ−2 and FMQ), whereas arc lavas have $\triangle\log fO_2$s ranging from FMQ to FMQ+6 (Christie et al., 1986; Carmichael, 1991). If these magma fO_2s directly reflect that of their mantle source regions, it must be concluded that sub-arc mantle is more oxidized than ambient asthenospheric mantle (Parkinson and Arculus, 1999). It is widely accepted that such oxidation is attributed to crustal metasomatism by fluids released from subducting oceanic crust. Many researchers suggest that oceanic subduction zone fluid is oxidized (Wood et al., 1990; Brandon and Draper, 1996; Arai et al., 2003), due to the high $Fe^{3+}/\sum Fe$ of altered oceanic crust (Rebay et al., 2010) and the significant mobility of Fe^{3+} that is preferentially incorporated into the fluid. Note that the mantle xenoliths in arc lavas have lower fO_2s (from FMQ−2 to FMQ+3) than arc lavas (Lee et al., 2005), probably implying that the mantle xenoliths do not represent the mantle source of arc lavas.

Relative to oceanic subduction zones, the oxygen fugacity of continental subduction zones has been given limited attention. Abundant studies have focused on the fO_2 of the SCLM peridotite xenoliths (McCammon et al., 2001; Woodland and Koch, 2003; McCammon and Kopylova, 2004; Frost and McCammon, 2008; Creighton et al., 2009; Wang J et al., 2013). However, less data are available on the fO_2 of garnet peridotites from the mantle wedge (Peslier et al., 2002; Malaspina et al., 2009b), resulting in unclear fO_2 modification effects of crustal metasomatism on the overlying mantle wedge. The fO_2 of ultramafic rocks can be calculated on the reactions among spinel/garnet, orthopyroxene and olivine. The redox equilibrium in spinel peridotite is $6Fe_2SiO_4$ (fayalite)$+O_2=2Fe_3O_4$ (magnetite in spinel)$+3Fe_2Si_2O_6$ (ferrosilite) (Mattioli and Wood, 1986; Wood and Virgo, 1989; Ballhaus et al., 1990, 1991), whereas that in garnet peridotite is $2Fe^{3+}{}_2Fe^{2+}{}_3Si_3O_{12}$ (skiagite in garnet)$=4Fe_2SiO_4$(fayalite)$+2Fe_2Si_2O_6$(ferrosilite)$+O_2$ (Luth et al., 1990; Gudmundsson and Wood, 1995; Woodland and Koch, 2003). In this paper, we calculated the fO_2s of the Dabie-Sulu orogenic peridotites based on the mineral compositions reported in the literature. As Fe^{3+} in garnet and spinel were calculated by assuming stoichiometry, the calculated results are semiquantitative.

To compare with other mantle environments, peridotites from various geological settings as well as MORBs are also shown in Figure 7. The peak stage fO_2s in the Dabie-Sulu orogenic peridotites have a wide range, from FMQ−5.5 to FMQ+1.75, and are negatively correlated with depth

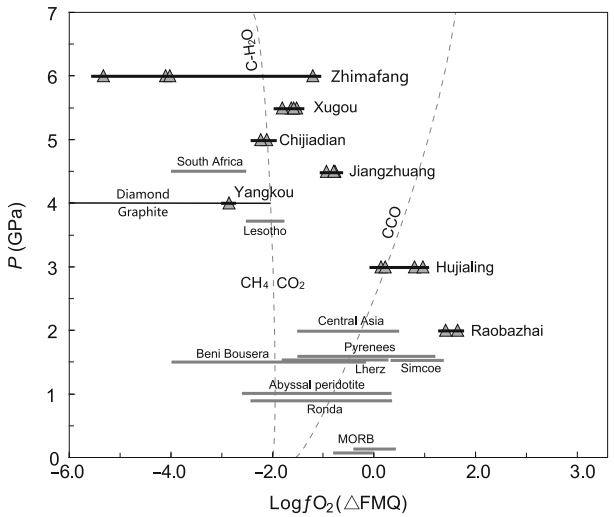

Figure 7 Ranges and average values of oxygen fugacity relative to FMQ for the Dabie-Sulu orogenic peridotites (black lines) as a function of pressure (depth) (modified after Frost and McCammon, 2008). They are compared with selected samples of spinel and garnet peridotites from various settings: oceanic mantle lithosphere (Bryndzia and Wood, 1990), spinel peridotite massifs (Woodland et al., 1992, 2006), garnet peridotite xenoliths from sub-cratonic mantle (Woodland and Koch, 2003) and spinel peridotite xenoliths from sub-arc mantle (Brandon and Draper, 1996; Parkinson and Arculus, 1999; Peslier et al., 2002). The CCO oxygen buffer ($C+O_2=CO_2$) and the C-H_2O join separating CH_4- and CO_2-rich aqueous fluids are from Malaspina et al. (2009b). The mineral compositions for the Dabie-Sulu orogenic peridotites are selected from the same literature as Figure 5. The oxygen fugacity of the Raobazhai peridotite is calculated by the olivine-orthopyroxene-spinel oxygen barometer (Ballhaus et al., 1991), whereas those of other garnet peridotites are calculated by the olivine-orthopyroxene-garnet oxygen barometer (Gudmundsson and Wood, 1995).

(Figure 7). Therefore, the mantle wedge above subducted continental crust becomes deoxidized at greater depths, which is consistent with the calculated results in cratonic mantle xenoliths (McCammon et al., 2001; Woodland and Koch, 2003) and HP-HT experiments (Rohrbach et al., 2007; Rohrbach and Schmidt, 2011). At the same depth, the mantle wedge above subducted continental crust appears to have higher oxygen fugacity than that of oceanic lithospheric mantle, SCLM and sub-arc mantle (Figure 7). Moreover, the Zhimafang garnet peridotite shows very low fO_2 at >4 GPa, which is consistent with the occurrence of diamond in the peridotite (Pan et al., 2003). However, the calculated results of oxygen fugacity are affected by many factors as follows. (1) The peak mineral compositions chosen for fO_2 calculations are different in samples collected from the same locality (e.g., Zhimafang), causing a large fO_2 discrepancy, up to 4 log units (Figure 8). (2) Magnetite, hematite, ilmenite, and chromite lamellae or rods are common in the Dabie-Sulu garnet peridotites (Zhang et al., 1999; Hwang et al., 2008). The formation of magnetite lamellae or rods was interpreted as exsolution of a peak spinel-solid solution Fe_3O_4-$(Fe, Mg)_2SiO_4$ (wadsleyite) during exhumation (Zhang et al., 1999) or dehydrogenation-oxidation of nominally anhydrous olivine during the early stage of exhumation (Hwang et al., 2008). However, the formation of magnetite-hematite rods or lamellae with both origins would directly decrease Fe^{3+} content in the peak olivine, resulting in underestimating the fO_2 results. (3) Dehydrogenation of garnet during exhumation would in crease

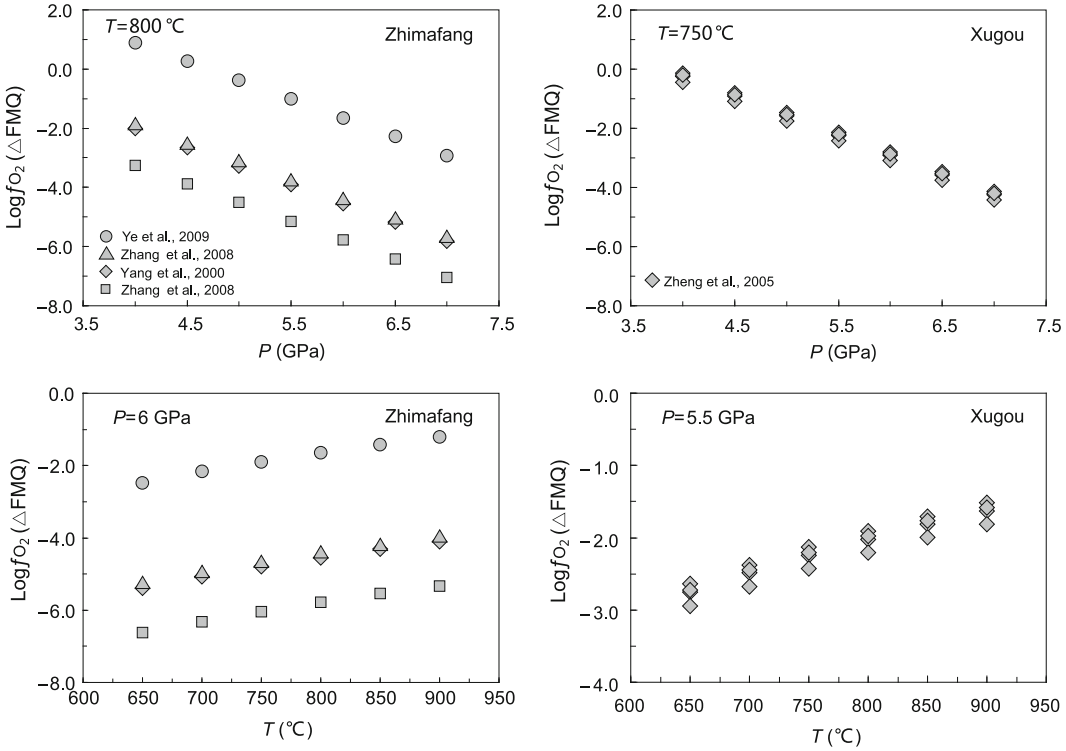

Figure 8 Effects of pressure, temperature and mineral composition on the calculated fO_2 (△FMQ) results.

"skiagite" activity (Ingrin and Skogby, 2000; McCammon et al., 2004). (4) The calculated fO_2 results are significantly affected by *P-T* conditions. In the Zhimafang garnet peridotite, 1 GPa and 100°C discrepancy will cause approximately 1.3 log units and 0.5 log units in fO_2 error, respectively (Figure 8).

Cratonic mantle xenoliths commonly have simple 4-phase (spinel-facies) or 5-phase (garnet-facies) mineral assemblages due to their high formation temperatures. They are also similar to the starting material used in experiments to construct fO_2 baraometries. Therefore, fO_2 baraometries are able to yield reliable results in the mantle xenoliths. However, orogenic peridotites have relatively complex mineral assemblages because of multistage metamorphism and metasomatism. Fe^{3+} contents distributed in minerals are highly heterogeneous. Revealing the effects of crustal-derived fluid/melt metasomatism on mantle oxygen fugacity requires us to carefully distinguish different stage metasomatic minerals. However, Fe^{3+} distribution in garnet, pyroxene and olivine is related not only to fO_2 but also to the equilibrated metasomatic minerals. Additionally, Fe^{3+} partitioning among the peridotite mineral phases under different *P-T* conditions is often neglected. Previous studies indicated that the $Fe^{3+}/\sum Fe$ in garnet was positively correlated with temperature (Canil and O'Neill, 1996; Woodland and Koch, 2003). The increase of Fe^{3+} in garnet with increasing temperature does not depend on the whole-rock $Fe^{3+}/\sum Fe$ but is rather the consequence of redistribution of Fe^{3+} from clinopyroxene into garnet (Canil and O'Neill, 1996). Therefore, the Fe^{3+} enrichment in garnet is not necessarily indicative of high whole-rock oxygen fugacity or the interaction with more oxidized metasomatic agents. Well-constrained interpretation of oxygen fugacity of the mantle wedge above the subducted continental crust should be based on exact ascertainment of the peridotite mineral textures, mineral assemblages, metamorphic stages and involved *P-T* conditions.

6 Prospects and conclusions

In the past twenty years, significant progress in mineralogy, petrology, protolith nature, petrochemistry, metamorphic and metasomatic evolution of the Dabie-Sulu orogenic peridotites has improved our understanding of mantle geodynamic processes and crust-mantle interactions. However, numerous key issues must be investigated further, such as complex phase relations constructed in the peridotite-pyroxenite system, mantle processes before subduction, element and isotope mobilization and fractionation during crust-mantle interactions, fO_2 modification during metasomatism by crust-derived C-O-H fluid/melt, and changes in the physical property of the mantle wedge during crustal metasomatism.

Phase relations in felsic-mafic rocks are now well constrained. However, both HP-HT experiments and thermodynamic modeling for ultramafic rocks have been only performed in a very simple system (Yang and Powell, 2008). Orogenic peridotites commonly have a complex composition due to the addition of various degrees of crustal components. It is necessary to construct phase relations in ultramafic rocks in complex systems, such as Ti- and Cr-bearing systems, which may help us understand mineral assemblages at different depths, mineral composition and proportions under given *P-T* conditions, and metamorphic *P-T* evolution of the rock. The key is to construct reliable composition-activity models for Cr-Ti-bearing spinel, garnet, pyroxene, phlogopite, Ti-clinohumite and Ti-chondrodite.

Most previous studies on orogenic peridotites focused on HP-UHP metamorphism and metasomatism during subduction; the mantle geodynamic processes that occur before subduction have been given little attention. The mantle processes prior to subduction include the mantle structure of the protoliths of orogenic peridotites, the partial melting and the melt-rock reaction processes. Most of the Dabie-Sulu orogenic peridotites record metamorphism before subduction, and some also present textures for silica-undersaturated melt-rock reactions prior to subduction. Understanding these mantle processes is a prerequisite to investigate crust-mantle interactions. *In situ* geochemical analyses of index textures will provide key information for understanding the mantle history of orogenic peridotites.

Element and isotope fractionations during crust-mantle interactions are always characterized by the formation of metasomatized veins or layers that systematically show diverse mineral assemblages, whole-rock major, trace and isotopic compositions. Determining the degrees of metasomatism requires us to understand the crust-derived fluid/melt compositions and the protolith nature of orogenic peridotites. Based on the degrees of metasomatism and the distance of metasomatized layers away from the protoliths, we are able to estimate which elements are more mobile, which elements are preferentially precipitated, and the internal relation between element and isotope fractionations.

The oxygen fugacity modification during crust-mantle interactions is also an important issue for further orogenic peridotite research. To investigate the effects of crustal metasomatism on the oxygen fugacity of the metasomatized mantle wedge, we should (1) accurately detect Fe^{3+} contents in garnet, spinel, olivine and pyroxene by using X-ray absorption near edge structure (XANES) or the 'Falnk method' technique with an electron microprobe (Höfer and Brey, 2007); (2) calculate different stage fO_2s based on careful discrimination of different stages of metasomatic minerals; (3) construct phase equilibrium relations on various whole rock $Fe^{3+}/\sum Fe$ to reveal the Fe^{3+} partitioning among the peridotite mineral phases under different *P-T* conditions; and (4) make a comparison between the calculated fO_2s and typical C-bearing phases in the peridotites, such as diamond, graphite, magnesite, CH_4 and CO_2.

The effects of crustal metasomatism on the physical properties (such as density, wave velocity, magnetoconductivity and electroconductibility) of the metasomatized mantle wedge remain enigmatic. Relative to the depleted mantle minerals, several newly formed minerals caused by modal metasomatism, such as phlogopite, amphibole, chlorite and talc, currently have lower densities and velocities but higher V_P/V_S ratios and seismic anisotropy. However, some metasomatic minerals, such as garnet, Fe-rich olivine and pyroxene, and Ti-clinohumite usually have higher densities and velocities but relatively lower seismic anisotropy. To constrain the physical properties of metasomatized mantle wedge rocks at different depths, we should establish the distribution of metasomatized minerals in the subduction factory at different depths, phase equilibrium relations and mineral evolution in peridotite-pyroxenite systems, and elastic parameters of related minerals. The investigations will provide direct petrological constraints on the physical property heterogeneity of the mantle.

We thank Prof. Zheng Yongfei for inviting us to write this paper. Special thanks are given to Profs. Li Shuguang, Zhang Lifei, Wei Chunjing, Liu Jingbo, Yang Jianjun, Jörg Hermann, Marco Scambelluri, Nadia Malaspina, Liu Liang, Li Qiuli, Liu Chuanzhou, and Wang Yongfeng. We also thank the three anonymous reviewers for their constructive comments on an earlier version. This work was supported by the National Basic Research Program of China (Grant No. 2015CB856103) and the National Natural Science Foundation of China (Grant Nos. 41090371 & 41372078).

Abbott J R N, Broman B N, Draper G. 2007. UHP magma paragenesis revisited, olivine clinopyroxenite and garnet-bearing ultramafic rocks from the Cuaba Gneiss, Rio San Juan Complex, Dominican Republic. Int Geol Rev, 49: 572–586

Ackerman L, Jelinek E, Medaris Jr G, et al. 2009. Geochemistry of Fe-rich peridotites and associated pyroxenites from Horni Bory, Bohemian Massif: Insights into subduction-related melt-rock reactions. Chem Geol, 259: 152–167

Ackerman L, Pitcher L, Strnad L, et al. 2013. Highly siderophile element geochemistry of peridotites and pyroxenites from Horni Bory, Bohemian Massif: Implications for HSE behaviour in subduction-related upper mantle. Geochim Cosmochim Acta, 100: 158–175

Agard P, Yamato P, Jolivet L, et al. 2009. Exhumation of oceanic blueschists and eclogites in subduction zones: Timing and mechanisms. Earth-Sci Rev, 92: 53–79

Arai S, Ishimaru S, Okrugin V. 2003. Metasomatized harzburgite xenoliths from Avacha volcano as fragments of mantle wedge of the Kamchatka arc: Implications for the metasomatic agent. Isl Arc, 12: 233–246

Arai S, Ishimaru S, Mizukami T. 2012. Methane and propane microinclusions in olivine in titanoclinohumite-bearing dunites from the Sanbagawa high-P metamorphic belt, Japan: Hydrocarbon activity in a subduction zone and Ti mobility. Earth Planet Sci Lett, 353-354: 1–11

Ballhaus C, Berry R F, Green D H. 1990. Oxygen fugacity controls in the Earth's upper mantle. Nature, 348: 437–440

Ballhaus C, Berry R F, Green D H. 1991. High pressure experimental calibration of the olivine-orthopyroxene-spinel oxygen geobarometer: Implications for the oxidation state of the upper mantle. Contrib Mineral Petrol, 107: 27–40

Barnes S J, Naldrett A J, Gorton M P, 1985. The origin of the fractionation of platinum-group elements in terrestrial magmas. Chem Geol, 53: 303–323

Becker H, Shirey S B, Carlson R W. 2001. Effects of melt percolation on the Re-Os systematics of peridotites from a Paleozoic convergent plate margin. Earth Planet Sci Lett, 188: 107–121

Becker H, Horan M, Walker R, et al. 2006. Highly siderophile element composition of the Earth's primitive upper mantle: Constraints from new data on peridotite massifs and xenoliths. Geochim Cosmochim Acta, 70: 4528–4550

Brandon A D, Draper D S. 1996. Constraints on the origin of the oxidation state of mantle overlying subduction zones: An example from Simcoe, Washington, USA. Geochim Cosmochim Acta, 60: 1739–1749

Braun M G, Kelemen P B. 2002. Dunite distribution in the Oman ophiolite: Implications for melt flux through porous dunite conduits. Geochem Geophys Geosyst, 3: 1–21

Beyer E E, Griffin W L, O'Reilly S Y. 2006. Transformation of Archaean lithospheric mantle by refertilization: Evidence from exposed peridotites in the Western Gneiss Region, Norway. J Petrol, 47: 1611–1636

Brenan J M, McDonough W F, Ash R. 2005. An experimental study of the solubility and partitioning of iridium, osmium and gold between olivine and silicate melt. Earth Planet Sci Lett, 237: 855–872

Brey G P, Doroshev A M, Girnis A V, et al. 1999. Garnet-spinel-olivine-orthopyroxene equilibria in the FeO-MgO-Al_2O_3-SiO_2-Cr_2O_3 system: I. Composition and molar volumes of minerals. Eur J Mineral, 11: 599–617

Brey G P, Bulatov V K, Girnis V. 2008. Geobarometry for Peridotites: Experiments in simple and natural systems from 6 to 10 GPa. J Petrol, 49: 3–24

Brueckner H K, Medaris L G. 2000. A general model for the intrusion and evolution of 'mantle' garnet peridotites in high-presssure and ultra-high-pressure metamorphic terranes. J Metamorph Geol, 18: 123–133

Brueckner H K, Van Roermund H L M, Pearson N J. 2004. An Archean(?) to Paleozoic evolution for a garnet peridotite lens with sub-Baltic Shield affinity within the Seve Nappe Complex of Jamtland, Sweden, central Scandinavian Caledonides. J Petrol, 45: 415–437

Bryant J A, Yogodzinski G M, Churikova T G. 2007. Melt-mantle interactions beneath the Kamchatka arc: Evidence from ultramafic xenoliths from Shiveluch volcano. Geochm Geophy Geosyst, 8, doi: 10.1029/2006GC001443

Bryndzia L T, Wood B K. 1990. Oxygen thermobarometry of abyssal spinel peridotites: The redox state and C-O-H volatile composition of the Earth's sub-oceanic upper mantle. Am J Sci, 290: 1093–1116

Büchl A, Brügmann G, Batanova V G, et al. 2002. Melt percolation monitored by Os isotopes and HSE abundances: A case study from the mantle section of the Troodos Ophiolite. Earth Planet Sci Lett, 204: 385–402

Canil D, O'Neill H S C. 1996. Distribution of ferric iron in some upper-mantle assemblages. J Petrol, 37: 609–635

Carmichael I S E. 1991. The redox states of basic and silicic magmas: A reflection of their source regions? Contrib Mineral Petrol, 106: 129–141

Carswell D A, Harvey M A, Alsamman A. 1983. The petrogenesis of contrasting Fe-Ti and Mg-Cr garnet peridotite types in the high-grade gneiss complex of Western Norway. Bull Mineral, 106: 727–750

Chalot-Prat F, Ganne J, Lombard A. 2003. No significant element transfer from the oceanic plate to the mantle wedge during subduction and exhumation of the Tethys lithosphere (Western Alps). Lithos, 69: 69–103

Chavagnac V, Jahn B M. 1996. Coesite-bearing eclogites from the Bixiling Complex, Dabie Mountains, China: Sm-Nd ages, geochemical characteristics and textonic implications. Chem Geol, 133: 29–51

Chazot G, Menzies M A, Harte B. 1996. Determination of partition coefficients between apatite, clinopyroxene, amphibole, and melt in natural spinel lherzolites from Yemen: Implications for wet melting of the lithospheric mantle. Geochim Cosmochim Acta, 60: 423–437

Christie D M, Carmichael I S E, Langmuir C H. 1986. Oxidation states of mid-ocean ridge basalt glasses. Earth Planet Sci Lett, 79: 397–411

Chen B, Jahn B M, Ye K, et al. 2002. Cogenetic relationship of the Yangkou gabbro-to-granite unit, Su-Lu terrane, eastern China, and implications for UHP metamorphism. J Geol Soc, 159: 457–467

Chen S Z, Yang J S, Xu Z Q, Li T F, Chen F Y. 2006a. Transformation of chromium spinel and garnet: Evidence of CCSD-PP3 ultramafic rocks processed UHP metamorphism (in Chinese). Earth Sci-J China Univ Geosci, 31: 475–487

Chen S Z, Yang J S, Zhong Z M. 2006b. Evidence of spinel facies partial

melting of the mantle rocks from the CCSD-PP3 drilling cores (in Chinese). Acta Petrol Sin, 22: 2815–2824
Chen Y, Ye K, Guo S, et al. 2013a. Multistage metamorphism of garnet orthopyroxenites from the Maowu mafic-ultramafic complex, Dabieshan UHP terrane, eastern China. Int Geol Rev, 55: 1239–1260
Chen Y, Ye K, Wu Y W, et al. 2013b. Hydration and dehydration in the lower margin of a cold mantle wedge: Implications for crust-mantle interactions and petrogeneses of arc magmas. Int Geol Rev, 55: 1506–1522
Chen Y, Ye K, Wu T F, et al. 2013c. Exhumation of oceanic eclogites: Thermodynamic constraints on pressure, temperature, bulk composition and density. J Metamorph Geol, 31: 549–570
Chen Y, Ye K, Su B, et al. 2013d. Metamorphic and metasomatic processes of the Dabie-Sulu orogenic peridotites (in Chinese). Chin Sci Bull, 58: 2294–2299
Chen Y, Ye K. 2013e. Exhumation of subducted oceanic crust: Key issues and discussion (in Chinese). Acta Petrol Sin, 29: 1461–1478
Coltorti M, Beccaluva L, Bonadiman C, et al. 2004. Amphibole genesis via metasomatic reaction with clinopyroxene in mantle xenoliths from Victoria Land, Antarctica. Lithos, 75: 115–139
Creighton S, Stachel T, Matveev S, et al. 2009. Oxidation of the Kaapvaal lithospheric mantle driven by metasomatism. Contrib Mineral Petrol, 157: 491–504
De Hoog J C M, Hattori K, Jung H. 2014. Titanium- and water-rich metamorphic olivine in high-pressure serpentinites from the Voltri Massif (Ligurian Alps, Italy): Evidence for deep subduction of high-field strength and fluid-mobile elements. Contrib Mineral Petrol, 167, doi: 10.1007/s00410-014-0990-x
Dick H J B, Bullen T. 1984. Chromian spinel as petrogenetic indicator in abyssal and alpine-type peridotites and spatially associated lavas. Contrib Mineral Petrol, 86: 54–76
Dobrzhinetskaya L, Green H W, Wang S. 1996. Alpe Arami: A peridotite massif from depths of more than 300 kilometers. Science, 271: 1841–1845
Doroshev A, Brey G, Girnis A, et al. 1997. Pyrope-knorringite garnets in the Earth's mantle: Experiments in the MgO-Al_2O_3-SiO_2-Cr_2O_3 system. Russ Geol Geophys, 38: 559–586
Enami M, Mizukami T, Yokoyama K. 2004. Metamorphic evolution of garnet-bearing ultramafic rocks from the Gongen area, Sanbagawa belt, Japan. J Metamorph Geol, 22: 1–15
Fleet M E, Crocket J H, Stone W E. 1996. Partitioning of platinum group elements (Os, Ir, Ru, Pt, Pd) and gold between sulfide liquid and basalt melt. Geochim Cosmochim Acta, 60: 2397–2412
Foley S F, Prelevic D, Rehfeldt T. 2013. Minor and trace elements in olivine as probes into early igneous and mantle melting process. Earth Planet Sci Lett, 363: 181–191
Frost D J, McCammon C A. 2008.The redox state of the Earth's mantle. Ann Rev Earth Planet Sci, 36: 389–420
Fu B, Touret J L R, Zheng Y F. 2003. Remnants of premetamorphic fluid and oxygen isotopic signitures in eclogites and garnet clinopyroxenite from the Dabie-sulu terranes, eastern China. J Metamorph Geol, 21: 561–578
Fumagalli P, Poli S. 2005. Experimentally determined phase relations in hydrous peridotite to 6.5 GPa and their consequences on the dynamics of subduction zones. J Petrol, 46: 555–578
Gao S, Rudnick R L, Carlson R W, et al. 2002. Re-Os evidence for replacement of ancient mantle lithosphere beneath the North China craton. Earth Planet Sci Lett, 198: 307–322
Garrido C J, Sanchez-Vizcaino V L, Gomez-Pugnaire M T, et al. 2005. Enrichment of HFSE in chlorite-harburgite produced by high-pressure dehydration of antigorite-serpentinite: Implications for subduction magmatism. Geochem Geophys Geosyst, 6, doi: 10.1029/2004GC 000791
Gasparik T, Newton R C. 1984. The reversed alumina contents of orthopyroxene in equilibrium with spinel and forsterite in the system MgO-Al_2O_3-SiO_2. Contrib Mineral Petrol, 85: 186–196
Griecoa G, Ferrarioa A, Mathezb E A. 2004. The effect of metasomatism on the Cr-PGE mineralization in the Finero Complex, Ivrea Zone, Southern Alps. Ore Geol Rev, 24: 299–314
Griffin W L, Shee S R, Ryan C G, et al. 1999. Harzburgite to lherzolite and back again: Metasomatic processes in ultramafic xenoliths from the Wesselton kimberlite, Kimberley, South Africa. Contrib Mineral Petrol, 134: 232–250
Griffin W L, O'Reilly S Y, Afonso J C, et al. 2009. The composition and evolution of lithospheric mantle: A re-evaluation and its tectonic implications. J Petrol, 50: 1185–1204
Girnis A V, Brey G P, Doroshev A M, et al. 2003. The system MgO-Al_2O_3-SiO_2-Cr_2O_3 revisited: Reanalysis of Doroshev et al.'s (1997) experiments and new experiments. Eur J Mineral, 15: 953–964
Gudmundsson G, Wood B J. 1995. Experimental tests of garnet peridotite oxygen barometry. Contrib Mineral Petrol, 119: 56–67
Guillot S, Hattori K H, Sigoyer J, et al. 2001. Evidence of hydration of the mantle wedge and its role in the exhumation of eclogites. Earth Planet Sci Lett, 193: 115–127
Guillot S, Hattori K, Agard P, et al. 2009. Exhumation processes in oceanic and continental subduction contexts: A review. In: Lallemand S, Funiciello F, eds. Subduction Zone Geodynamics. Berlin-Heidelberg: Springer. 175–205
Haggerty S Y. 1995. Upper mantle mineralogy. J Geodynam, 20: 331–364
Hattori K H, Guillot S. 2007. Geochemical character of serpentinites associated with high- to ultrahigh-pressure metamorphic rocks in the Alps, Cuba, and the Himalayas: Recycling of elements in subduction zones. Geochem Geophy Geosyst, 8, doi: 10.1029/2007GC001594
Hattori K H, Wallis S, Enami M, et al. 2010a. Subduction of mantle wedge peridotites: Evidence from the Higashi-akaishi ultramafic body in the Sanbagawa metamorphic belt. Isl Arc, 19: 192–207
Hattori K H, Guillot S, Saumur B M, et al. 2010b. Corundum-bearing garnet peridotite from northern Dominican Republic: A metamorphic product of an arc cumulate in the Caribbean subduction zone. Lithos, 114: 437–450
Hermann J, Rubatto D, Trommsdorff V. 2006. Sub-solidus Oligocene zircon formation in garnet peridotite during fast decompression and fluid infiltration (Duria, Central Alps). Mineral Petrol, 88: 181–206
Höfer H E, Brey G P. 2007. The iron oxidation state of garnet by electron microprobe: Its determination with the flank method combined with major-element analysis. Am Mineral, 92: 873–885
Hwang S L, Yui T F, Chu H T, et al. 2008. Hematite and magnetite precipitates in olivine from the Sulu peridotite: A result of dehydrogenation-oxidation reaction of mantle olivine? Am Mineral, 93: 1051–1060
Iizuka Y, Nakamura E. 1995. Experimental study of the slab-mantle interaction and implications for the formation of titanoclinohumite at deep subduction zone. Proceed Jap Acad, 71: 159–164
Ingrin J, Skogby H. 2000. Hydrogen in nominally anhydrous upper-mantle minerals: Concentration levels and implications. Eur J Mineral, 12: 543–570
Ionov D A, Hofmann A W. 1995. Nb-Ta-rich mantle amphiboles and micas: Implications for subduction-related metasomatic trace element fractionations. Earth Planet Sci Lett, 131: 341–356
Jahn B M, Fan Q C, Yang J J, et al. 2003. Petrogenesis of the Maowu pyroxenite-eclogite body from the UHP metamorphic terrane of Dabieshan: Chemical and isotopic constraints. Lithos, 70: 243–267
John T, Scambelluri M, Frische M, et al. 2011. Dehydration of subducting serpentinite: Implications for halogen mobility in subduction zones and the deep halogen cycle. Earth Planet Sci Lett, 308: 65–76
Kalfoun F, Ionov D, Merlet C. 2002. HFSE residence and Nb/Ta ratios in metasomatised rutile-bearing mantle peridotites. Earth Planet Sci Lett, 199: 49–65
Katayama I, Muko A, Iizuka T, et al. 2003. Dating of zircon from Ti-clinohumite-bearing garnet peridotite: Implication for timing of mantle metasomatism. Geology, 31: 713–716
Kelemen P B. 1990. Reaction between ultramafic rock and fractionating basaltic magma I. Phase relations, the origin of calc-alkaline magma series, and the formation of discordant dunite. J Petrol, 31: 51–98
Kelemen P B, Dick H J B. 1995. Focused melt flow and localized deformation in the upper-mantle: Juxtaposition of replacive dunite and ductile shear zones in the Josephine peridotite, SW Oregon. J Geophys Res, 100: 423–438
Kendrick M A, Scambelluri M, Honda M, et al. 2011. High abundances of

noble gas and chlorine delivered to the mantle by serpentinite subduction. Nature Geosci, 4: 807–812
Keppler H. 1993. Influence of fluorine on the enrichment of high field strength trace elements in granitic rocks. Contrib Mineral Petrol, 114: 479–488
Klemme S, O'Neill H S C. 2000. The near-solidus transition from garnet lherzolite to spinel lherzolite. Contrib Mineral Petrol, 138: 237–248
Klemme S. 2004. The influence of Cr on the garnet-spinel transition in the Earth's mantle: Experiments in system MgO-Cr_2O_3-SiO_2 and thermodynamic modeling. Lithos, 77: 639–646
Klemme S, Ivanic T J, Connolly J A D, et al. 2009. Thermodynamic modelling of Cr-bearing garnets with implications for diamond inclusions and peridotite xenoliths. Lithos, 112: 986–991
Kodolányi J, Pettke T, Spandler C, et al. 2012. Geochemistry of ocean floor and fore-arc serpentinites: Constraints on the ultramafic input to subduction zones. J Petrol, 53: 235–270
Kress V C, Carmichael I S E. 1991. The compressibility of silicate liquids containing Fe_2O_3 and the effect of composition, temperature, oxygen fugacity and pressure on their redox states. Contrib Mineral Petrol, 108: 82–92
Krogh E J, Carswell D A. 1995. HP and UHP eclogites and garnet peridotites in the Scandinavian Caledonides. In: Coleman R G, Wang X, eds. Ultrahigh Pressure Metamorphism. Cambridge: Cambridge University Press. 244–298
Kubo K. 2002. Dunite formation processes in highly depleted peridotite: Case study of the Iwanaidake peridotite, Hokkaido, Japan. J Petrol, 43: 423–448
Le Roux V, Bodinier J L, Tommasi A, et al. 2007. The Lherz spinel lherzolite: Refertilized rather than pristine mantle. Earth Planet Sci Lett, 259: 599–612
Lee C T A, Leeman W P, Canil D, et al. 2005. Similar V/Sc systematics in MORB and arc basalts: Implications for the oxygen fugacities of their mantle source regions. J Petrol, 46: 2313–2336
Lee C T A, Luffi P, Le Roux V, et al. 2010. The redox state of arc mantle using Zn/Fe systematics. Nature, 468: 681–685
Li X P, Rahn M, Bücher K. 2004. Serpentinites of the Zermatt-Saas ophiolite complex and their texture evolution. J Metamorph Geol, 22: 159–177
Li X P, Yang J S, Robinson P, et al. 2011. Petrology and geochemistry of UHP-metamorphosed ultramafic-mafic rocks from the main hole of the Chinese Continental Scientific Drilling Project (CCSD-MH), China: Fluid/melt-rock interaction Mafic-ultramafic complex from CCSD-MH. J Asi Earth Sci, 42: 661–683
Liang Y, Sun C, Yao L. 2013. A REE-in-two-pyroxene thermometer for mafic and ultramafic rocks. Geochim Cosmochim Acta, 102: 246–260
Liati A, Gebauer D. 2009. Crustal origin of zircon in a garnet peridotite: A study of U-Pb SHRIMP dating, mineral inclusions and REE geochemistry (Erzgebirge, Bohemian Massif). Eur J Mineral, 21: 737–750
Liou J G, Zhang R Y. 1998. Petrogenesis of an ultrahigh-pressure garnet-bearing ultramafic body from Maowu, Dabie Mountains, eastern-central China. Isl Arc, 7: 115–134
Liou J G, Tsujimori T, Zhang R Y, et al. 2004. Global UHP metamorphism and continental subduction/collision: the Himalayan model. Int Geol Rev, 46: 1-27
Liu F L, Shi J R, Liu J H, et al. 2011. Protolith and ultrahigh-pressure (UHP) metamorphic ages of ultramafic rocks in Weihai area, North Sulu UHP terrane (in Chinese). Acta Petrol Sin, 27: 1075–1084
Liu J G, Rudnick R L, Walker R J, et al. 2010. Processes controlling highly siderophile element fractionations in xenolithic peridotites and their influence on Os isotopes. Earth Planet Sci Lett, 297: 287–297
Liu J G, Rudnick R L, Walker R J, et al. 2011. Mapping lithospheric boundaries using Os isotopes of mantle xenoliths: An example from the North China Craton. Geochim Cosmochim Acta, 75: 3881–3902
Liu J G, Rudnick R L, Walker R J, et al. 2014. Big insights from tiny peridotites: Evidence for persistence of Precambrian lithosphere beneath the eastern North China Craton. Tectonophysics, DOI: 10.1016/j.tecto.2014.05.009
Liu Q, Hou Q L, Xie L W, et al. 2012. Different origins of the fractionation of platinum-group elements in Raobazhai and Bixiling Mafic-ultramafic rocks from the Dabie Orogen, central China. J Geol Res, doi: 10.1155/2012/631426
Liu Y S, Zong K Q, Kelemen P B, et al. 2008. Geochemistry and magmatic history of eclogites and ultramafic rocks from the Chinese continental scientific drill hole: Subduction and ultrahigh-pressure metamorphism of lower crustal cumulates. Chem Geol, 247: 133–153
Lorand J P, Luguet A, Alard O, et al. 2008. Abundance and distribution of platinum-group elements in orogenic lherzolites: A case study in a Fontete Rouge lherzolite (French Pyrénées). Chem Geol, 248: 174-194
Lorand J P, Luguet A, Alard O. 2013. Platinum-group element systematics and petrogenetic processing of the continental upper mantle: A review. Lithos, 164-167: 2–21
Louvel M, Sanchez-Valle C, Malfait W J, et al. 2013. Zr complexation in high pressure fluids and silicate melts and implications for the mobilization of HFSE in subduction zones. Geochim Cosmochim Acta, 104: 281–299
Luth R W, Virgo D, Boyd F R, et al. 1990. Ferric iron in mantle-derived garnets: Implications for thermobarometry and for the oxidation state of the mantle. Contrib Mineral Petrol, 104: 56–72
Malaspina N, Hermann J, Scambelluri M, et al. 2006. Polyphase inclusions in garner-orthopyroxenite (Dabie Shan, China) as monitors for metasomatism and fluid-related trace element transfer in subduction zone peridotite. Earth Planet Sci Lett, 249: 173–187
Malaspina N, Hermann J, Scambelluri M. 2009a. Fluid/mineral interaction in UHP garnet peridotite. Lithos, 107: 38–52
Malaspina N, Poli S, Fumagalli P. 2009b. The oxidation state of metasomatized mantle wedge: Insights from C-O-H bearing garnet peridotite. J Petrol, 50: 1533–1552
Mattioli G S, Wood B J. 1986. Upper mantle oxygen fugacity recorded by spinel lherzolites. Nature, 322: 626–628
McCammon C A, Griffin W L, Shee S R, et al. 2001. Oxidation during metasomatism in ultramafic xenoliths from the Wesselton kimberlite, South Africa: Implications for the survival of diamond. Contrib Mineral Petrol, 141: 287–296
McCammon C A, Forst D J, Smyth J R, et al. 2004. Oxidation state of iron in hydrous mantle phases: Implications for subduction and mantle oxygen fugacity. Phys Earth Planet Int, 143-144: 157–169
McCammon C A, Kopylova M G. 2004. A redox profile of the Slave mantle and oxygen fugacity control in the cratonic mantle. Contrib Mineral Petrol, 148: 55–68
McDonough W F, Sun S S. 1995. The composition of the Earth. Chem Geol, 120: 223–253
McPherson E, Thirlwall M F, Parkinson I J, et al. 1996. Geochemistry of metasomatism adjacent to amphibole-bearing veins in the Lherz peridotite massif. Chem Geol, 134: 135–157
Medaris Jr G, Wang H, Jelínek E, et al. 2005. Characteristics and origins of diverse Variscan peridotites in the Gföhl nappe, Bohemian Massif, Czech Republic. Lithos, 82: 1–23
Melcher F, Grum W, Simon G, et al. 1997. Petrogenesis of the ophiolitic giant chromite deposits of Kempirsai, Kazakhstan: A study of solid and fluid inclusions in chromite. J Petrol, 38: 1419–1458
Mellini M, Rumori C, Viti C. 2005. Hydrothermally reset magmatic spinels in retrograde serpentinites: Formation of ''ferritchromit'' rims and chlorite aureoles. Contrib Mineral Petrol, 149: 266–275
Menzies M A, Vannucci R, Bodinier J L. 2001. Orogenic lherzolites and mantle processes. J Petrol, 42: 3–4
Miller D P, Marschall H R, Schumacher J C. 2009. Metasomatic formation and petrology of blueschist-facies hybrid rocks from Syros (Greece): Implications for reactions at the slab-mantle interface. Lithos, 107: 53–67
Morgan Z, Liang Y. 2005. An experimental study of the kinetics of lherzolite reactive dissolution with applications to melt channel formation. Contrib Mineral Petrol, 150: 369–385
Nozaka T. 2003. Compositional heterogeneity of olivine in thermally metamorphosed serpentinite from southwest Japan. Am Mineral, 88: 1377–1384
O'Neill H S C. 1981. The transition between spinel lherzolite and garnet lherzolite, and its use as a geobarometer. Contrib Mineral Petrol, 77: 185–194

Padrón-Navarta J A, Hermann J, Garrido C J, et al. 2010. An experimental investigation of antigorite dehydration in natural silica-enriched serpentinite. Contrib Mineral Petrol, 159: 25–42
Padrón-Navarta J A, López S V, Garrido C J, et al. 2011. Metamorphic record of high-pressure dehydration of antigorite serpentinite to chloritic harzburgite in a subduction setting (Cerrodel Almirez, Nevado-Filabride Complex, southern Spain). J Petrol, 52: 2047–2078
Pan M B, Zhang Q L, Lu H F, et al. 2003. The discovery of diamond from the Zhimafang pyrope peridotite the Sulu UHP Metamorphic Zone, East China. Acta Geol Sinica, 77: 332–337
Parkinson I J, Arculus R J. 1999. The redox state of subduction zones: Insights from arc-peridotites. Chem Geol, 160: 409–423
Pearce J A, Barker P F, Edwards S J, et al. 2000. Geochemistry and tectonic significance of peridotites from the South Sandwich arc-basin system, South Atlantic. Contrib Mineral Petrol, 139: 36–53
Peslier A H, Luhr J F, Post J. 2002. Low water contents in pyroxenes from spinel peridotites of the oxidized, sub-arc mantle wedge. Earth Planet Sci Lett, 201: 69–86
Piccardo G B, Vissers R L M. 2007. The pre-oceanic evolution of the Erro-Tobbio peridotite (Voltri Massif, Ligurian Alps, Italy). J Geodyn, 43: 417–449
Powell W, Zhang M, O'Reilly S Y, et al. 2004. Mantle amphibole trace-element and isotopic signatures trace multiple metasomatic episodes in lithospheric mantle, western Victoria, Australia. Lithos, 75: 141–171
Rajesh V J, Arai S, Satish-kumar M, et al. 2013. High-Mg low-Ni olivine cumulates from a Pan-African accretionary belt in southern India: Implications for the genesis of volatile-rich high-Mg melts in suprasubduction setting. Precambrian Res, 227: 409–425
Rapp R P, Shimizu N, Norman M D, et al. 1999. Reaction between slab-derived melts and peridotite in the mantle wedge: Experimental constraints at 3.8 GPa. Chem Geol, 160: 335–356
Rapp J F, Klemme S, Butler I B, et al. 2010. Extremely high solubility of rutile in chloride and fluoride-bearing metamorphic fluids: An experimental investigation. Geology, 38: 323–326
Rebay G, Powell R, Diener F A. 2010. Calculated phase equilibria for a MORB composition in a *P-T* range, 450–650°C and 18–28 kbar: The stability of eclogite. J Metamorph Geol, 28: 635–645
Rebay G, Spalla M I, Zanoni D. 2012. Interaction of deformation and metamorphism during subduction and exhumation of hydrated oceanic mantle: Insights from the Western Alps. J Metamorph Geol, 30: 687–802
Reverdatto V V, Selyatitskiy A Y, Carswell D A. 2008. Geochemical distinctions between 'crustal' and mantle-derived peridotites/pyroxenites in high/ultrahigh pressure metamorphic complexes. Russ Geol Geophy, 49: 73–90
Righter K, Campbell A J, Humayun M, et al. 2004. Partitioning of Ru, Rh, Pd, Re, Ir and Au between Cr-bearing spinel, olivine, pyroxene and silicate melts. Geochim Cosmochim Acta, 68: 867–880
Rohrbach A, Ballhaus C, Schindler U G, et al. 2007. Metal saturation in the upper mantle. Nature, 449: 456–458
Rohrbach A, Schmidt, M W. 2011. Redox freezing and melting in the Earth's deep mantle resulting from carbon-iron redox coupling. Nature, 472: 209–212
Santos J F, Scharer U, Ibarguchi J I G, et al. 2002. Genesis of pyroxenite-rich peridotite at Cabo Ortegal (NW Spain): Geochemical and Pb-Sr-Nd isotope data. J Petrol, 43: 17–43
Savov I P, Ryan J G, D'Antonio M, et al. 2005. Geochemistry of serpentinized peridotites from the Mariana Forearc Conical Seamount, ODP Leg 125: Implications for the elemental recycling at subduction zones. Geochem Geophys Geosyst, 6, doi: 10.1029/2004GC000777
Savov I P, Ryan J G, D'Antonio M, et al. 2007. Shallow slab fluid release across and along the Mariana arc-basin system: Insights from geochemistry of serpentinized peridotites from the Mariana fore arc. J Geophys Res, 112, doi: 10.1029/2006JB004749
Scambelluri M, Bottazzi P, Trommsdorff V, et al. 2001. Incompatible element-rich fluids released by antigorite breakdown in deeply subducted mantle. Earth Planet Sci Lett, 192: 457–470
Scambelluri M, Müntener O, Ottolini L, et al. 2004. The fate of B, Cl and Li in the subducted oceanic mantle and in the antigorite-breakdown fluids. Earth Planet Sci Lett, 222: 217–234
Scambelluri M, Hermann J, Morten L, et al. 2006. Melt- versus fluid-induced metasomatism in spinel to garnet wedge peridotites (Ulten Zone, Eastern Italian Alps): Clues from trace element and Li abundances. Contrib Mineral Petrol, 151: 372–394
Scambelluri M, Pettke T, van Roemund H L M. 2008. Majoritic garnets monitor deep subduction fluid flow and mantle dynamics. Geology, 36: 59–62
Scambelluri M, Herman L M, Roemund V, et al. 2010. Mantle wedge peridotites: Fossil reservoirs of deep subduction zone processes: Inferences from high and ultrahigh-pressure rocks from Bardane (Western Norway) and Ulten (Italian Alps). Lithos, 120: 186–201
Scambelluri M, Pettke T, Rampone E, et al. 2014. Petrology and trace element budgets of high-pressure peridotites indicate subduction dehydration of serpentinized mantle (Cima di Gagone, central Alps, Switzerland). J Petrol, 55: 459–498
Shaw C S J, Heidelbach F, Dingwell D B. 2006. The origin of reaction textures in mantle peridotite xenoliths from Sal Island, Cape Verde: The case for "metasomatism" by the host lava. Contrib Mineral Petrol, 151: 681–697
Shen T T, Hermann J, Zhang L F, et al. 2014. FTIR spectroscopy of Ti-chondrodite, Ti-clinohumite, and olivine in deeply subducted serpentinites and implications for the deep water cycle. Contrib Mineral Petrol, 167, doi: 10.1007/s00410–014–0992–8
Song S G, Su L, Niu Y L, et al. 2009. CH_4 inclusions in orogenic harzburgite: Evidence for reduced slab fluids and implication for redox melting in mantle wedge. Geochim Cosmochim Acta, 73: 1737–1754
Spandler C, Pirard C. 2013. Element recycling from subducting slabs to arc crust: A review. Lithos, 170: 208–223
Spengler D, van Roermund H L M, Drury M R, et al. 2006. Deep origin and hot melting of an Archaean orogenic peridotite massif in Norway. Nature, 440: 913–917
Spengler D, Obata M, Hirajima T, et al. 2012. Exsolution of garnet and clinopyroxene from high-Al pyroxenes in Xugou peridotite, eastern China. J Petrol, 53: 1477–1504
Suhr G, Hellebrand E, Snow J E, et al. 2003. Significance of large, refractory dunite bodies in the upper mantle of the Bay of Islands Ophiolite. Geochem Geophys Geosyst, 4, doi: 10.1029/2001gc000277
Sun C, Liang Y. 2014. An assessment of subsolidus re-equilibration on REE distribution among mantle minerals olivine, orthopyroxene, clinopyroxene, and garnet in peridotites. Chem Geol, 372: 80–91
Sun W D, Arculus R J, Kamenetsky V S, et al. 2004. Release of gold-bearing fluids in convergent margin magmas prompted by magnetite crystallization. Nature, 431: 975–978
Tang Y J, Zhang H F, Ying J F, et al. 2013. Widespread refertilization of cratonic and circum-cratonic lithospheric mantle. Earth Sci Rev, 118: 45–68
Tatsumi Y. 1986. Formation of the volcanic front in subduction zones. Geophys Res Lett, 13: 717–720
Thompson R N, Gibson S A. 2000. Transient high temperatures in mantle plume heads inferred from magnesian olivines in Phanerozoic picrites. Nature, 407: 502–506
Trommsdroff V, Risold A C, Reusser E, et al. 2001. Titanian clinohumite: Ilmenite rod inclusions and phase relations (abstract), Central Alps. Paper presented at Workshop on Fluid/Slab/Mantle Interactions and UHP Minerals, Waseda University, Tokyo. 84
Tsai C H, Liu J G, Ernst G. 2000. Petrological characterization and tectonic significance of retrogressed garnet peridotites, Raobazhai area, North Dabie Complex, east-central China. J Metamorph Geol, 18: 181–192
Tursack E, Liang Y. 2012. A comparative study of melt-rock reactions in the mantle: Laboratory dissolution experiments and geological field observations. Contrib Mineral Petrol, 163: 861–876
Uysal İ, Ersoy E Y, Dilek Y et al. 2015. Depletion and refertilization of the Tethyan oceanic upper mantle as revealed by the early Jurassic Refahiye ophiolite, NE Anatolia-Turkey. Gondwana Res, 27: 594–611
van Achterbergh E, Griffin W L, Stiefenhofer J. 2001. Metasomatism in mantle xenoliths from the Letlhakane kimberlites: Estimation of element fluxes. Contrib Mineral Petrol, 141: 397–414

Vrijmoed J C, Van Roermund H L M, Davies G R. 2006. Evidence for diamond-grade ultra-high pressure metamorphism and fluid interaction in the Svartberget Fe-Ti garnet peridotite-websterite body, Western Gneiss Region, Norway. Mineral Petrol, 88: 381–405

Vrijmoed J C, Austrheim H, John T, et al. 2013. Metasomatism in the Ultrahigh-pressure Svartberget Garnet-peridotite (Western Gneiss Region, Norway): Implications for the Transport of Crust-derived Fluids within the Mantle. J Petrol, 54: 1815–1848

Wang J, Hattori K H, Kilian R, et al. 2007. Metasomatism of sub-arc mantle peridotites below southernmost South America: Reduction of fO_2 by slab-melt. Contrib Mineral Petrol, 153: 607–624

Wang J, Hattori K, Xu W, et al. 2012. Origin of ultramafic xenoliths in high-Mg diorites from east-central China based on their oxidation state and abundance of platinum group elements. Int Geol Rev, 54: 1203–1218

Wang J, Hattori K, Xie Z P. 2013. Oxidation state of lithospheric mantle along the northeastern margin of the North China Craton: Implications for geodynamic processes. Int Geol Rev, 55: 1418–1444

Wang X B, Yang J J, Chen S Y, et al. 2005. Origin and structure nature of Raobazhai ultramafic rock: A discussion (in Chinese). Acta Petrol Sin, 21: 1593–1608

Wang Z C, Becker H, Gawronski T. 2013. Partial re-equilibration of highly siderophile elements and the chalcogens in the mantle: A case study on the Baldissero and Balmuccia peridotite massifs (Ivrea Zone, Italian Alps). Geochim Cosmochim Acta, 108: 21–44

Walter M, Katsura T, Kubo A, et al. 2002. Spinel-garnet lherzolite transition in the system CaO-MgO-Al_2O_3-SiO_2 revisited: An *in situ* X-ray study. Geochim Cosmochim Acta, 66: 2109–2121

Wilke M, Schmidt C, Dubrail J, et al. 2012. Zircon solubility and zirconium complexation in H_2O+Na_2O+SiO_2±Al_2O_3 fluids at high pressure and temperature. Earth Planet Sci Lett, 349-350: 15–25

Wood B J, Virgo D. 1989. Upper mantle oxidation state: Ferric iron contents of lherzolite spinels by 57Fe Mössbauer spectroscopy and resultant oxygen fugacities. Geochim Cosmochim Acta, 53: 1277–1291

Wood B J, Bryndzia L T, Johnson K E. 1990. Mantle oxidation state and its relationship to tectonic environment and fluid speciation. Science, 248: 337–345

Woodland A B, Kornprobst J, Wood B J. 1992. Oxygen thermobarometry of orogenic lherzolite massifs. J Petrol, 33: 203–230

Woodland A B, Koch M. 2003. Variation in oxygen fugacity with depth in the upper mantle beneath the Kaapvaal craton, Southern Africa. Earth Planet Sci Lett, 214: 295–310

Woodland A B, Kornprobst J, Tabitc A. 2006. Ferric iron in orogenic lherzolite massifs and controls of oxygen fugacity in the upper mantle. Lithos, 89: 222–241

Wu F Y, Walker R J, Yang Y H, et al. 2006. The chemical-temporal evolution of lithospheric mantle underlying the North China Craton. Geochim Cosmochim Acta, 70: 5013–5034

Xie Z P, Hattori K, Wang J. 2013. Origins of ultramafic rocks in the Sulu Ultrahigh-pressure Terrane, Eastern China. Lithos, 178: 158–170

Xu S T, Okay A I, Ji S. 1992. Diamond from the Dabie Shan metamorphic rocks and its implication for tectonic setting. Science, 256: 80–82

Xu S T, Liu Y, Chen G, et al. 2003. New finding of micro-diamands in eclogites from Dabie-Sulu region in central-eastern China. Chin Sci Bull, 48: 988–994

Xu S T, Liu Y C, Chen G B, et al. 2005. Microdiamonds, their classification and tectonic implications for the host eclogites from the Dabie and Su-Lu regions in central eastern China. Mineral Mag, 69: 509–520

Xu W L, Hergt J M, Gao S, et al. 2008. Interaction of adakitic melt-peridotite: Implications for the high-$Mg^{\#}$ signature of Mesozoic adakitic rocks in the eastern North China Craton. Earth Planet Sci Lett, 265: 123–137

Xu W L, Yang D B, Gao S, et al. 2010. Geochemistry of peridotite xenoliths in Early Cretaceous high $Mg^{\#}$ diorites from the central Orogenic Block of the North China Craton: The nature of Mesozoic lithospheric mantle and constraints on lithospheric thinning. Chem Geol, 270: 257–273

Xue F, Rowley D B, Baker J. 1996. Refolded syn-ultrahigh-pressure thrust sheets in the south Dabie complex, China: Field evidence and tectonic implications. Geology, 5: 455–458

Yang J J, Jahn B M. 2000. Deep subduction of mantle-derived garnet peridotites from the Su-Lu UHP metamorphic terrane in China. J Metamorph Geol, 18: 167–180

Yang J J. 2003. Titanian clinohumite–garnet–pyroxene rock from the Su-Lu UHP metamorphic terrane, China: Chemical evolution and tectonic implications. Lithos, 70: 359–379

Yang J J. 2006. Ca-rich garnet-clinopyroxene rocks at Hujialin in the Su-Lu Terrane (eastern China): Deeply subducted arc cumulates? J Petrol, 47: 965–990

Yang J J, Powell R. 2008. Ultrahigh-pressure garnet peridotites from the devolatilization of sea-floor hydrated ultramafic rocks. J Metamorph Geol, 26: 695–716

Yang J J, Huang M X, Naemura K. 2013. Towards a law for the metamorphic evolution of mantle-derived orogenic peridotites (in Chinese). Acta Petrol Sin, 29: 1479–1485

Yang J S, Wooden J L, Wu C L, et al. 2003. SHRIMP U-Pb dating of coesite-bearing zircon from the ultrahigh-pressure metamorphism rocks, Sulu terrane, East China. J Metamorph Geol, 21: 551–560

Yang J S, Chen S Z, Zhang Z M, et al. 2005. A preliminary study of the Chinese Continental Scientific Drilling (CCSD) PP3 hole on the Gangshang garnet peridotite body in the Sulu UHPM belt (in Chinese). Acta Petrol Sin, 21: 293–304

Yang J S, Zhang R Y, Li T F, et al. 2007. Petrogenesis of the garnet peridotite and garnet-free peridotite of the Zhimafang ultramafic body in the Sulu ultrahigh pressure metamorphic belt, eastern China. J Metamorph Geol, 25: 187–206

Yang J S, Li T F, Chen S Z, et al. 2009. Genesis of garnet peridotites in the Sulu UHP belt: Examples from the Chinese continental scientific drilling project-main hole, PP1 and PP3 drill holes. Tectonophysics, 475: 359–382

Ye K, Liu J B, Cong B L, et al. 2001. Overpressures induced by coesite-quartz transition in zircon. Am Mineral, 86: 1151–1155

Ye K, Song Y R, Chen Y, et al. 2009. Multistage metamorphism of orogenic garnet-lherzolite from Zhimafang, Sulu UHP terrane, E. China: Implications for mantle wedge convection during progressive oceanic and continental subduction. Lithos, 109: 155–175

Yu Y, Xu W L, Wang C G. 2014. Experimental studies of melt-peridotite reactions at 1–2 GPa and 1250–1400°C and their implications for transforming the nature of lithospheric mantle and for high-Mg signatures in adakitic rocks. Sci China Earth Sci, 57: 415–427

Yuan H L, Gao S, Rudnick R L, et al. 2007. Re-Os evidence for the age and origin of peridotites from the Dabie-Sulu ultrahigh pressure metamorphic belt, China. Chem Geol, 236: 323–338

Zenetti A, Mazzucchelli M, Rivalenti G, et al. 1999. The Finero phlogopite-peridotite massif: An example of subduction-related metasomatism. Contrib Mineral Petrol, 134: 107–122

Zhang C, van Roermund H, Zhang L F. 2011. Orogenic garnet peridotites: Tools to reconstruct Paleo-geodynamic settings of fossil continental collision zones. In: Dobrzhinetskaya L F, Faryad S W, Wallis S, et al., eds. Ultrahigh Pressure Metamorphism: 25 Years After the Discovery of Coesite and Diamond. London: Elsevier Insights. 501–540

Zhang H F, Sun M, Lu F X, et al. 2001. Geochemical significance of a garnet lherzolite from the Dahongshan kimberlite, Yangtze Craton, southern China. Geochem J, 35: 315–331

Zhang H F, Sun M, Zhou X H, et al. 2003. Secular evolution of the lithosphere beneath the eastern North China Craton: evidence from Mesozoic basalts and high-Mg andesites. Geochim Cosmochim Acta, 67: 4373–4387

Zhang H F, Goldstein S L, Zhou X H, et al. 2008. Evolution of subcontinental lithospheric mantle beneath eastern China: Re-Os isotopic evidence from mantle xenoliths in Paleozoic kimberlites and Mesozoic basalts. Contrib Mineral Petrol, 155: 271–293

Zhang R Y, Liou J G, Cong B L. 1995. Talc-, magnesite- and Ti-clinohumite-bearing ultrahigh-pressure meta-mafic and ultramafic complex in the Dabie Mountains, China. J Petrol, 36: 1011–1037

Zhang R Y, Liou J G. 1998. Dual origin of garnet peridotites of Dabie-Sulu UHP terrane, eastern-central China. Episodes, 21: 229–234

Zhang R Y, Shu J F, Mao H K, et al. 1999. Magnetite lamellae in olivine

and clinohumite from Dabie UHP ultramafic rocks, central China. Am Mineral, 84: 564–569
Zhang R Y, Liou J G, Yang J S, et al. 2000. Petrochemical constraints for dual origin of garnet peridotites from the Dabie-Sulu UHP terrane, eastern-central China. J Metamorph Geol, 18: 149–166
Zhang R Y, Liou J G, Yang J S, et al. 2004. Garnet peridotites in UHP mountain belts of China. Int Geol Rev, 46: 981–1004
Zhang R Y, Yang J S, Wooden J L, et al. 2005a. U-Pb SHRIMP geochronology of zircon in garnet peridotite from the Sulu UHP terrane, China: Implication for mantle metasomatism and subduction-zone UHP metamorphism. Earth Planet Sci Lett, 237: 729–734
Zhang R Y, Liou J G, Zheng J P, et al. 2005b. Petrogenesis of the Yangkou layered garnet-peridotite complex, Sulu UHP terrane, China. Am Mineral, 90: 801–813
Zhang R Y, Liou J G, Tsujimori T, et al. 2006. Non UHP unit in the Sulu UHP terrane, eastern China: Transformation of Proterozoic granulite and gabbro to garnet amphibolite. In: Hacker B R, McClelland B, Liou J G, eds. Ultrahigh-Pressure Metamorphism: Deep Continental Subduction. Mineral Petrol, 88: 169–206
Zhang R Y, Li T, Rumble D, et al. 2007. Multiple metasomatism in Sulu ultrahigh-*P* garnet peridotite constrained by petrological and geochemical investigations. J Metamorph Geol, 25: 149–164
Zhang R Y, Pan Y M, Yang Y H, et al. 2008. Chemical composition and ultrahigh-*P* metamorphism of garnet peridotites from the Sulu UHP terrane, China: Investigation of major, trace elements and Hf isotopes of minerals. Chem Geol, 255: 250–264
Zhang R Y, Liou J G, Ernst W G. 2009. The Dabie-Sulu continental collision zone: A comprehensive review. Gondwana Res, 16: 1–29
Zhang R Y, Jahn B M, Liou J G, et al. 2010. Origin and tectonic implication of an UHP metamorphic mafic-ultramafic complex from the Sulu UHP terrane, eastern China: Evidence from petrological and geochemical studies of CCSD-Main Hole core samples. Chem Geol, 276: 69–87
Zhang R Y, Liou J G, Huberty J M, et al. 2011. Origin and metamorphic evolution of garnet clinopyroxenite from the Sulu UHP terrane, China: Evidence from mineral chemistry and microstructures. In: Dobrzhinetskaya L F, Faryad S W, Wallis S, et al., eds. Ultrahigh Pressure Metamorphism: 25 Years After the Discovery of Coesite and Diamond. London: Elsevier Insights. 151–185
Zhang Z M, Liou J G, Zhao S, et al. 2006. Petrogenesis of Maobei Fe-Ti rich eclogites from the Southern Sulu UHP metamorphic belt, east-central China. J Metamorph Geol, 24: 727–741
Zhang Z M, Dong X, Liou J G, et al. 2011. Metasomatism of garnet peridotite from Jiangzhuang, southern Sulu UHP belt: Constraints on the interactions between crust and mantle rocks during subduction of continental lithosphere. J Metamorph Geol, 29: 917–937
Zhao R, Zhang R Y, Liou J G, et al. 2007. Petrochemistry, oxygen isotopes and U-Pb SHRIMP geochronology of mafic-ultramafic bodies from the Sulu UHP terrane, China. J Metamorph Geol, 25: 207–224
Zheng Y F, Yang J J, Gong B, Jahn B M. 2003. Partial equilibrium of radiogenic and stable isotope systems in garnet peridotite during ultrahigh-pressure metamorphism. Am Mineral, 88: 1633–1643
Zheng J P, Sun M, Zhou M F, et al. 2005a. Trace elemental and PGE geochemical constraints of Mesozoic and Cenozoic peridotitic xenoliths on lithospheric evolution of the North China Craton. Geochim Cosmochim Acta, 69: 3401–3418
Zheng J P, Zhang R Y, Griffin W L, et al. 2005b. Heterogeneous and metasomatized mantle recorded by trace elements in minerals of the Donghai garnet peridotites, Sulu UHP terrane, China. Chem Geol, 221: 243–259
Zheng J P, Griffin W L, O'Reilly S Y, et al. 2006a. A refractory mantle protolith in younger continental crust, east-central China: Age and composition of zircon in the Sulu ultrahigh-pressure peridotite. Geology, 34: 705–708
Zheng J P, Griffin W L, O'Reilly S Y, et al. 2006b. Mineral chemistry of peridotites from Paleozoic, Mesozoic and Cenozoic lithosphere: Constraints on mantle evolution beneath eastern China. J Petrol, 47: 2233–2256
Zheng J P, Sun M, Griffin W L, et al. 2008. Age and geochemistry of contrasting peridotite types in the Dabie UHP belt, eastern China: Petrogenetic and geodynamic implications. Chem Geol, 247: 282–304
Zheng J P, Tang H Y, Xiong Q, et al. 2014. Linking continental deep subduction with destruction of a cratonic margin: Strongly reworked North China SCLM intruded in the Triassic Sulu UHP belt. Contrib Mineral Petrol, 168: doi: 10.1007/s00410-014-1028-0
Zheng L, Zhi X C, Reisberg L. 2009. Re-Os systematics of the Raobazhai peridotite massifs from the Dabie orogenic zone, eastern China. Chem Geol, 268: 1–14
ZhengY F, Xia Q X, Chen R X, Gao X Y. 2011. Partial melting, fluid supercriticality and element mobility in ultrahigh-pressure metamorphic rocks during continental collision. Earth Sci Rev, 107: 342–374
Zheng Y F. 2012. Metamorphic chemical geodynamics in continental subduction zones. Chem Geol, 328: 5–48
Zheng Y F, Zhao Z F, Chen Y X. 2013. Continental subduction channel processes: Plate interface interaction during continental collision. Chin Sci Bull, 58: 4371–4377
Zheng Y F, Hermann J. 2014. Geochemistry of continental subduction-zone fluids. Earth Planets Space, 66: 93
Zhi X C, Jin Y B, Meng Q, et al. 2004. Trace element geochemistry of Raobazhai ultramafic complex, North Dabie Mountain (in Chinese). Acta Petrol Sin, 20: 463–472
Ziberna L, Klemme S, Nimis P. 2013. Garnet and spinel in fertile and depleted mantle: Insights from thermodynamic modelling. Contrib Mineral Petrol, 166: 411–421
Zotov N, Keppler H. 2000. *In-situ* Raman spectra of dissolved silica species in aqueous fluids to 900°C and 14 kbar. Am Mineral, 85: 600–603